A novel bispecific ligand-directed toxin designed to simultaneously target EGFR on human glioblastoma cells and uPAR on tumor neovasculature

A THESIS
SUBMITTED TO THE FACULTY OF THE GRADUATE SCHOOL
OF THE UNIVERSITY OF MINNESOTA
BY

Alexander K. Tsai

IN PARTIAL FULFILLMENT OF THE REQUIREMENTS
FOR THE DEGREE OF
MASTER OF SCIENCE

Dr. Daniel A. Vallera

September, 2010

Table of Contents

Page(s)

List of Figures…….…….ii-iii

List of Tables……..iv

Abbreviations……...v-vi

Overview……1-2

Literature Review…….....3-12

1. Glioblastoma Multiforme…….…..3
2. Angiogenesis…….....3-4
3. Targeted Toxins……...4-5
4. Bispecific Ligand-Directed Toxins…….…...5
5. Epidermal Growth Factor & Receptor…….....…..6-8
6. Urokinase Plasminogen Activator & Receptor……..…….....8-10
7. Diphtheria Toxin……..10
8. Pseudomonas Exotoxin……...…10-11
9. Immunogenicity……..11-12

Materials and Methods……..…13-20

1. Construction of targeted toxins……...……...…..13-14
2. Isolation of inclusion bodies, refolding, and purification……...……...……...14
3. Cell culture…….……16
4. Flow cytometry analysis of EGFATFKDEL……16-17
5. Bioassays to measure cell proliferation……17-18
6. Determining immunogenicity of deimmunized EGFATFKDEL 7mut in mice……...18
7. Maximum tolerated dose of EGFATFKDEL and monospecifics…….19
8. *In vivo* efficacy studies of EGFATFKDEL 7mut against U87 flank tumors...19-20
9. Statistical analysis……..20

Results……..21-63

1. Toxicity of DTEGFATF and EGFATFKDEL against GBM……21
2. Toxicity of DTEGFATF and EGFATFKDEL against endothelial cells……...26
3. Activity of EGF and ATF targeting ligands……..29
4. Binding of EGFATFKDEL to U87 cells……...32
5. Reducing the immunogenicity of EGFATFKDEL…….…..…34-35, 40, 42
6. Maximum Tolerated Dose of EGFATFKDEL……..44
7. *In vivo* efficacy of EGFATFKDEL 7mut against U87-Luc flank tumors…...46, 53

Discussion……63-71

Bibliography……72-81

Figures

Page

Figure 1. Gene map for EGFATFKDEL 7mut……15

Figure 2A. Effect of DTEGFATF on $EGFR^{+}$/$uPAR^{+}$ U87 cells…….…….22

Figure 2B. Effect of DTEGFATF on U87-Luc cells……23

Figure 2C. Effect of EGFATFKDEL on U87 cells……..24

Figure 2D. Effect of EGFATFKDEL on U87-Luc cells……...25

Figure 3A. Effect of DTEGFATF on HUVEC……27

Figure 3B. Effect of EGFATFKDEL on HUVEC……28

Figure 4A. Activity on both targeting ligands in DTEGFATF……30

Figure 4B. Activity of both targeting ligands in EGFATFKDEL 7mut……31

Figure 5. Ability for EGFKDEL, ATFDEL, and EGFATFKDEL to bind to U87 cells…….……33

Figure 6A. Activity of deimmunized EGFATFKDEL 7mut ……36

Figure 6B. Activity of EGFATFKDEL 7mut in U87-Luc cells……37

Figure 6C. Effect of EGFATFKDEL 7mut on HUVEC……38

Figure 6D. Specificity of EGFATFKDEL 7mut……39

Figure 7. Immunogenicity of a mutated TT, EGFATFKDEL 7mut……43

Figure 8A. Average tumor volumes in the first experiment……..47

Figure 8B. Average body weights in the first experiment……48

Figure 9A. Bioluminescent images in untreated mice of first experiment……49

Figure 9B. Bioluminescent images of treated mice in the first experiment……50

Page

Figure 10A. Bioluminescent measurements of untreated mice in the first experiment……51

Figure 10B. Bioluminescent measurements of treated mice in the first experiment……52

Figure 11A. Average tumor volumes in the second experiment……..54

Figure 11B. Average body weights in the second experiment……..55

Figure 12A. Bioluminescent images of untreated mice in the second experiment……56

Figure 12B. Bioluminescent images of 2219ARLKDEL mice in the second experiment……57

Figure 12C. Bioluminescent images of EGFATFKDEL 7mut mice in the second experiment……58

Figure 13A. Bioluminescent measurements of untreated mice in the second experiment……59

Figure 13B. Bioluminescent measurements of 2219ARLKDEL mice in the second experiment……60

Figure 13C. Bioluminescent measurements of EGFATFKDEL 7mut mice in the second experiment……61

Figure 13D. Bioluminescent measurements of ATFKDEL mice in the second experiment……62

Tables

Page

Table 1: Cytotoxicity…….41

Table 2: Deaths / Total Animals……..……..45

Abbreviations

APC	Antigen presenting cell
ATF	Amino-terminal fragment
BBB	Blood brain barrier
BCPC	Brain cancer propagating cell
BLT	Bispecific ligand-directed toxin
CED	Convection enhanced delivery
DT	Diphtheria toxin
EF2	Elongation factor 2
EGF	Epidermal growth factor
EGFR	Epidermal growth factor receptor
ER	Endoplasmic reticulum
FITC	Fluorescein isothiocyanate
GBM	Glioblastoma multiforme
GPI	Glycosylphosphatydilinositol
HMA	Human muscle adolase
HNSCC	Head and neck squamous cell carcinoma
HUVEC	Human umbilical vein endothelial cell
i.p	Intraperitoneal
IC	Intracranial
IC_{50}	Inhibitory concentration 50%
IP3	Inositoltriphosphate
IPTG	Isopropyl-b-D-thiogalactopyranoside
Luc	Luciferase
mAb	Monoclonal antibody
MAP/ERK	Mitogen-activated protein-kinase extracellular signal-regulated kinase
MHC	Major histocompatibility complex
MMP	Matrix metalloprotease
MTD	Maximum tolerated dose
NAD	Nicotinomide adenine dinucleotide

PAI-1	Plasminogen activator inhibitor 1
PAI-2	Plasminogen activator inhibitor 2
PE	Pseudomonas exotoxin
PKC	Protein kinase C
RTK	Receptor tyrosine kinase
STAT	Signal transducer activator of transcription
suPAR	Soluble urokinase plasminogen activator receptor
TKI	Tyrosine kinase inhibitor
tPA	Tissue plasminogen activator
TT	Targeted Toxin
uPA	Urokinase plasminogen activator (urokinase)
uPAR	Urokinase plasminogen activator receptor
VEGF	Vascular endothelial growth factor

Overview

Targeted toxins (TTs) are a class of therapeutic molecules directed against human cancer. By directing TTs toward cancer specific targets using tumor reactive ligands, they can be designed to be selective against numerous cancer types. Because TTs are designed to specifically destroy cancerous cells without damaging healthy cells, their potential outweighs most of the non-specific therapies such as chemotherapy and radiotherapy currently used in cancer patients. Recently, the potential of TTs has grown in the field of cancer research through continuous improvement using genetic engineering. Thorough preclinical studies of TTs are important for the characterization of TT biology, identification of possible solutions to TT drawbacks, and the development of novel TTs. Studies have led to several clinical trials, some of which have displayed promising results and confirmed the potential of TTs in cancer therapy.

To date, most TTs attack cancer using a single targeting molecule. Two novel drugs, DTEGFATF and EGFATFKDEL that are the subject of this thesis, are unique in that they are bispecific ligand-directed toxins (BLTs), and are designed to simultaneously target both solid tumors and their associated neovasculature. DTEGFATF is a diphtheria toxin (DT) containing BLT, while EGFATFKDEL is a pseudomonas exotoxin (PE) containing BLT. Both BLTs target two receptors, epidermal growth factor receptor (EGFR) and urokinase plasminogen activator receptor (uPAR), which are commonly overexpressed on the cell surface of several different cancers. uPAR-targeting was used because it is overexpressed not only on solid tumors, but also on the neovasculature. We observed that the two BLTs possessed similar *in vitro* biological properties and activities because DT and PE have identical mechanisms of action. Additionally, by modifying certain amino acids on the PE molecule in EGFATFKDEL, we were able to produce a novel third agent, EGFATFKDEL 7mut, which possesses significantly reduced immunogenicity while maintaining activity. The efficacy of a TT is dependent on the ability to give multiple courses of treatment, and the production of neutralizing antibodies against TTs has historically been a major limitation in TT clinical trials. By modifying

PE and targeting dual markers, we were able to produce a novel TT with impressive anti-tumor activity against glioblastoma *in vitro* and *in vivo*.

Literature Review

1. Glioblastoma Multiforme

Gliomas are cancers that originate from glial cells in the brain or central nervous system. Astrocytomas are a subset of gliomas in which malignant cells resemble astrocytes. Glioblastoma multiforme (GBM), the most common and malignant of all primary intracranial (IC) malignancies, is defined by the World Health Organization as a grade IV astrocytoma[1,2]. Over a third of all primary brain tumors are gliomas, and one half of these are GBM[1]. Most GBM cases occur in older individuals and are primary (de novo) in nature, while secondary glioblastomas (generally arising from low-grade astrocytomas) account for fewer GBM cases and usually occur in younger individuals[3].

After diagnosis, generally via CT scanning or MRI, the current treatment standard begins with aggressive surgical resection[1]. Previously, radiotherapy alone was the standard treatment, but a recent randomized clinical trial using radiotherapy with concomitant and adjuvant treatment with the chemotherapeutic agent, temozolomide, suggests that this combined treatment is superior to radiotherapy alone[4,5]. Still, the median survival time using concomitant chemotherapy increased only modestly by 2.6 months[4]. Thus, despite advancements in both radiotherapy and chemotherapy, the prognosis for GBM patients remains poor. Sadly, the cost of treatment versus improvement in quality-adjusted life-years is the highest in the U.S[6]. Consequently, several alternative treatment strategies are currently being explored. Biological agents, such as targeted toxins are attractive for GBM treatment because glioblastoma rarely metastasizes outside of the cranium. As a result, TTs may be applicable to GBM through direct administration to tumors via convection enhanced delivery (CED), a method that utilizes catheters and pumps to deliver drugs directly to the tumor site[7-9].

2. Angiogenesis

One of the critical requirements for tumor growth is angiogenesis – the growth of new blood vessels from pre-existing vessels. Without an adequate nutrient and oxygen supply, tumors can only grow to limited size. Additionally, angiogenesis is believed to

play roles in tumor invasiveness and metastasis[10]. Angiogenesis is a complex process. A variety of different factors, ranging from metabolic stress to genetic mutation, can signal for or against angiogenesis. The balance of these factors is crucial in deciding if angiogenesis will occur[11]. Moreover, endothelial cells, stromal cells, and factors from the extracellular matrix are all involved in the process itself. The number of variables involved in angiogenesis has made it challenging to study[11]. However, research in anti-angiogenics is still conducted because the inhibition of angiogenesis should effectively reduce tumor growth and metastasis. To a great extent, observing angiogenesis has been hampered by the limitations of PET, CT, and MRI imaging techniques. Recently, intravital microscopy, which offers the ability to observe subcellular details in living tissue, has allowed improved visualization of tumor neovasculature[10]. The neovasculature differs from normal blood vessels both structurally and functionally. The blood vessels supplying tumors contract abnormally, are highly disorganized, and highly permeable[10,11]. Therapeutically, these features restrict the targeting and modulation of tumor neovasculature. However, because adhesion molecules and other cell surface markers are overexpressed on neovasculature, therapies targeting these markers have been popular and successful[11]. Today, the most widely used marker is vascular endothelial growth factor (VEGF), but several other strategies exist. The most successful anti-angiogenic, bevacizumab (Avastin) – a monoclonal antibody targeting VEGF – has been FDA approved for treatment in combination with chemotherapy of non small-cell lung cancer, breast cancer, and colorectal cancer[12]. In addition, numerous anti-angiogenic drugs are currently in clinical trials[11].

3. Targeted Toxins

Targeted toxins, also referred to as immunotoxins, cytotoxins, or fusion proteins are a broad class of biologicals which deliver a naturally derived toxin to a specific tissue. TTs are usually composed of a bacteria- or plant-derived toxin which is linked to some type of targeting ligand(s). While in research, TTs have only recently become popular, their basic concept is derived from the work of Paul Ehlrich during the early 20th century[13]. However, it took over half a century for Ehlrich's concepts to reach fruition

when antibodies were introduced as a viable option to guide toxins toward their targets[14]. Recognition of this targeting strategy has increased in the past decades, and while still in its infancy, the development of TTs continues to progress.

About 35 years after their introduction as targeting molecules, antibodies remain the most popular choice when selecting a targeting ligand for TTs. Yet, several other strategies exist. The most common of these alternatives include using growth factors, natural ligands of human receptors, and cytokines of the immune system. Use of these newer methods has allowed for a broader spectrum of targets and arguably more effective targeting.

The toxin portion of TTs has remained relatively consistent. Toxin selection is generally straightforward because most toxins simply kill cells and the method by which a toxin initiates cell death is usually unimportant. However, there are some differences, perhaps the most important of which is potency, which are generally taken into account. Toxins are usually derived from plants (ricin or gelonin) or bacteria (Pseudomonas exotoxin or diphtheria toxin). All of these toxins kill cells by inhibiting protein production – either by disrupting ribosome formation or by hampering translation[14].

The development of TTs continues to move forward and their popularity has recently increased. Today, while only a few TTs have been approved for clinical use, several clinical trials have been or are being conducted[14].

4. Bispecific Ligand-Directed Toxins

The concept of using two targeting entities on a single TT was developed in the early 1990s[15-17]. A similar technique has also been used in the creation of bispecific monoclonal antibodies[18]. Bispecific ligand-directed toxins (BLTs) contain two unique targeting ligands which are linked to a bacterial toxin fragment on a single chain[19,20]. The use of the two different targeting molecules clearly increases targeting potential, but less obvious benefits have also been discovered. BLTs have been demonstrated to possess enhanced anti-tumor activity and superior binding, while also being less toxic[19,21-26].

5. Epidermal Growth Factor & Receptor

In 1962, the epidermal growth factor (EGF) ligand was discovered in mice by Stanley Cohen[27,28]. In the following years, Cohen's laboratory discovered the human EGF homolog and studied various forms of the ligand. However, the group was not able to isolate the approximately 170 kDa epidermal growth factor receptor (EGFR) until 1980[29,30]. In the following three decades, EGF, EGFR, and other similar receptors would become potent targets for the treatment of cancer and other diseases.

Upon binding by EGF, EGFR activates pathways which lead to either cell differentiation or proliferation[29]. Several other ligands, including transforming growth factor-α, amphiregulin, heparin-binding EGF-like growth factor, vaccinia virus growth factor, and betacellulin have been identified which bind to EGFR[29,31]. These ligands contain six cysteine residues which, in combination with three disulfide bonds, form the structural basis required for binding to EGFR[28]. The extracellular portion of EGFR contains four domains, only one of which is involved in ligand binding. The intracellular section of EGFR contains a tyrosine kinase which autophosphorylates EGFR and phosphorylates several cellular substrates involved in downstream signal transduction pathways. Binding by the EGF ligand induces a conformational change in the receptor which increases kinase activity. Phosphorylation primarily activates the classic mitogen-activated protein kinase extracellular signal-regulated kinase (MAPK/ERK) proliferation signaling pathway. Other targets include phospholipase C-γ which can activate protein kinase C (PKC) and inositoltriphosphate (IP3) production. As is common in other receptors, the receptor-ligand complex is endocytosed and either degraded or recycled[29,32]. More recent research has suggested an alternative and more direct nuclear signaling method, at least in cancer cells and other rapidly dividing cells[33-36]. The presence of EGFR in the nuclei of these cells suggests a mechanism in which the receptor tyrosine kinase (RTK) is imported into the nucleus. Further research has made this mechanism more plausible by demonstrating EGFR's ability to interact with nuclear transcription factors and by using examples of other RTKs which can be localized to the nucleus[36].

While the mutation and overexpression of EGFR has been identified in several different malignant cancers including various lung, colorectal, breast, esophageal, bladder, and ovarian cancers, EGFR's role in cancer was first discovered in glioblastoma[29,31,37-40]. In cancer, EGFR is believed to play a central role in tumor growth and development[29]. Many mutations in EGFR have been identified, but they are not always common in particular cancers[31]. More often, gene amplification occurs, and when the EGFR protein is modified, it is usually due to alternative splicing[29,31]. Even when mutations cause constitutive activation of the tyrosine kinase, as is the case with the common EGFRvIII intragenic rearrangement mutation, the overactivity of EGFR is often thought to be overshadowed by the overexpression of the constitutively activated receptor[29]. The level of EGFR overexpression has commonly been used as a predictor for poor clinical outcome, but its success as such a predictor has been mixed and dependent on the subset of carcinoma examined[41-44]. In any case, the overexpression or overactivity of EGFR clearly adds to the malignant phenotype in cancers.

EGFR's presence on a number of different cancers, and the belief that it often plays a central role in malignancy, has made it a popular target when designing potential treatments for cancer therapy. Today, three strategies, tyrosine kinase inhibitors (TKIs), monoclonal antibodies (mAbs), and targeted toxins, are the most common methods to combat cancer via EGFR targeting. Small proteins which are aimed to hinder the autophosphorylation of EGFR are perhaps the most well known EGFR inhibitors. Gefitinib and erlotinib, both TKIs, are approved for non-small cell lung carcinoma patients who have previously been treated with chemotherapy. Erlotinib has also recently been approved for treatment of pancreatic cancer patients. These TKIs have shown great promise in a small subset of patients, but their clinical use has remained primarily experimental. Further randomized clinical studies are needed to determine the potential of TKIs under various conditions and when applied during different periods of tumor progression and treatment[39,45]. In clinical trials with GBM patients, ertlotinib treatment has been promising, while responses to gefitinib have been disappointing[32]. There are also two FDA approved mAb drugs: cetuximab and panitumumab. Both are approved for colorectal cancer, and cetuximab has also been approved for treatment of certain head

and neck cancers. The results of clinical trials in EGFR mAbs have been similar to TKIs, and while promising, need more research[46,47]. Currently, no TTs aimed at EGFR in cancer have been approved for clinical use. However, several TTs are currently in clinical trials and many more are in preclinical studies[48,49].

6. Urokinase Plasminogen Activator & Receptor

The urokinase plasminogen activator system is primarily involved in the complex process of fibrinolysis and tissue remodeling, but it has also been implicated in processes such as cell migration, adhesion, and proliferation[50-52]. The system includes two activating ligands, urokinase plasminogen activator – also known as urokinase (uPA) – and tissue plasminogen activator (tPA), both of which are serine proteases that bind to identical receptors. Additional components include urokinase plasminogen activator receptor (uPAR), a three-domain glycosylphosphatydilinositol (GPI)-anchored receptor, and two inhibitors, plasminogen activator inhibitor 1 and 2 (PAI-1 and PAI-2). The single chain zymogen, pro-uPA, must be converted by plasmin to the active two-chain urokinase which has enzymatic activity. Several alternate proteases, such as cathepsin B or L, plasma kallikrein, nerve growth factor-γ, and mast cell tryptase are also known to activate pro-uPA[53]. The active urokinase induces the activation of plasminogen by converting it to plasmin. Plasmin then degrades fibrin which prevents the buildup of extracellular matrix. This pathway plays a role in the degradation of clots as well as tissue remodeling[50]. It is important to recognize that both tPA and uPA act directly on plasminogen to activate it without any interaction with uPAR. In fact, fibrinolysis was unaffected in double uPAR-knockout mice[54]. However, multiple members of the fibrinolysis pathway, including plasmin and matrix metalloproteases (MMPs), can cleave and alter uPAR – indicating some involvement of the receptor in fibrinolysis[55-57]. Additionally, it is thought that binding of uPA and uPAR increases its exposure to membrane-bound plasminogen[53].

The uPA system's involvement in cell migration and adhesion directly relates it to both innate and adaptive immunity. Inflammatory responses due to bacterial infections lead to the increased production of uPA in several cell lines[58]. Urokinase may then recruit

and activate neutrophils via interactions with uPAR[50]. uPAR-dependent cell migration and adhesion is thought to be primarily regulated through integrins and signaling pathways such as MAPK/ERK and Janus kinase-signal transducer and activator of transcription (STAT)[59]. The role of the uPA system in adaptive immunity is less clear, but overwhelming evidence suggests that urokinase and its receptor participate in the activation of T cells. uPAR is expressed on naïve T cells and several different antigen-presenting cells (APCs), and the levels of uPAR expression often change during different stages of T cell development[60-63]. Moreover, studies have shown that mice deficient in elements of the uPA system respond poorly when challenged with pathogens[64-67].

In 1985, Francesco Blasi separated the binding and catalytic portions of urokinase[68,69]. Incubation of intact urokinase in a solution at pH 8 results in cleavage of the molecule at the amino acid position 135. The amino-terminal fragment (ATF) contains amino acids 1-135, and is capable of binding to uPAR, but does not contain the remaining carboxy-terminus fragment which confers proteolytic activity[69-70]. ATF has been shown to bind with high affinity to uPAR (K_d = 0.5 nM)[71]. Upon binding, the ATF/uPAR complex primarily remains bound to the cell surface without being internalized[69]. Naturally, the uPA/uPAR complex must bind to PAI-1 or PAI-2 before being internalized. However, it has been shown that linking ATF to other translocation-conferring domains can result in internalization[71]. This trait has led to ATF's inclusion in TTs.

The upregulation of components of the uPA system has been discovered in numerous cancers. Associations have been made with breast, ovarian, gastrointestinal, lung, brain, kidney, bladder, and soft tissue cancers[53]. At first, the uPA system's roles in cell migration and tissue remodeling were believed to correspond with a few distinct metastatic characteristics such as cancer cell migration and angiogenesis. The latter has been of particular interest because anti-angiogenic drugs, at least in principle, seem to have such impressive potential. While vascular endothelial growth factor (VEGF) has been the most popular target in anti-angiogenics due to its association with virtually all steps in angiogenesis, the uPA system, because of its role in endothelial cell invasion, is also a viable target[72]. Moreover, uPAR's overexpression on both the tumor and its

neovasculature in some cancers has made it a more attractive targeting system[73,74]. More recently, uPA and uPAR have been found to be involved in tumor cell proliferation, adhesion, migration, invasion, and growth at the metastatic site[75]. This overall involvement has made the uPAR system a popular target in designing drugs to target the many malignancies which overexpress urokinase and uPAR.

The three domain uPAR receptor can be cleaved into several different soluble forms (suPAR) by a number of different molecules. Three forms of soluble uPAR can be isolated from blood. The first is an intact uPAR molecule, suPAR(I-III). Cleavage between the first and second domains produces the remaining soluble forms, suPAR(I) and suPAR(II-III)[51]. In research, blood measurements of suPAR and urokinase have been used to predict prognoses of ovarian, breast, and colorectal cancer patients, and while relationships have been found, they have rarely been conclusive enough to use clinically[51,76,77]. Thus, the value of uPAR as a biomarker may not be as valuable as its use in biological targeting strategies.

7. Diphtheria Toxin

Diphtheria toxin (DT) is a bacterial toxin produced by *Corynebacterium diphtherae* which is commonly used in the construction of targeted toxins. DT causes diphtheria in humans[78]. The toxin is a 58 kDa 535 amino acid exotoxin which consists of three domains: a binding domain, translocation domain, and a catalytic domain[14,78]. DT targets elongation factor 2 (EF2) and disrupts this factor's involvement in translation which results in inhibition of protein synthesis. More specifically, the toxin transfers ADP-ribose derived from nicotinomide adenine dinucleotide (NAD) to EF2 to inhibit its activity. DT is extremely potent. Just a single molecule of DT delivered to the cytosol is sufficient to induce cell death[79]. TTs can be produced from DT by truncating the toxin to only its catalytic domain and linking the truncated portion to targeting ligand(s)[14,80].

8. Pseudomonas Exotoxin

Pseudomonas exotoxin (PE) is a 613 amino acid produced by *Pseudomonas aeruginosa* which is highly related to DT. Like DT, PE contains three domains,

inactivates EF2 to inhibit protein synthesis, and is extremely potent. Just 1000 molecules of PE internalized into tumor cells can result in a complete tumor regression[81].

There has been significant development and modification of PE for use in TTs. In the early 1990s, it was discovered that modification of amino acids 609-613 in PE from Arg-Glu-Asp-Leu-Lys (REDLK) to the endoplasmic reticulum (ER) retention signal, Lys-Asp-Glu-Leu (KDEL), dramatically increased cytotoxicity[82,83]. Normally, the terminal lysine of the REDLK sequence is cleaved, which results in a REDL sequence that can interact with KDEL receptors. This interaction allows transfer from the Golgi apparatus to the ER, where the toxin can translocate to the cytosol. It is believed that transport via REDL is relatively inefficient, and that the KDEL modification enhances transfer to the ER[83,84]. Since its discovery, the KDEL modification has commonly been used in TTs which employ PE.

Further modification to PE has recently been developed which effectively reduces the immunogenicity of the toxin. In 2006, through topographical epitope mapping, Onda and Pastan identified seven B cell epitopes of PE38 – the commonly used truncated form of PE[85]. Onda and Pastan further demonstrated that mutation of eight amino acids spanning each of the seven epitopes would result in a PE38 fragment that was significantly less immunogenic in mice, but still maintained cytotoxicity[86]. This more recent discovery combined with the earlier KDEL modification has made PE a popular and effective toxin choice in TT development.

9. Immunogenicity

Immunogenicity is the propensity for a substance to induce an immune response. Today, the importance of monitoring immunogenicity has grown as targeted therapies become more popular for virtually all diseases. The development of targeted toxins in particular has been slowed by immunogenicity[87]. The effectiveness of TTs hinges on the ability to give multiple or sustained treatments[80]. However, because the toxins used in TTs are non-mammalian in origin, administration of TTs inevitably leads to the generation of neutralizing antibodies which dramatically reduce or eliminate TT efficacy[85,88]. Importantly, these antibodies are almost always directed at the toxin portion

of TTs and are even produced in environments such as the brain[80,85,88]. In fact, 73% of patients treated using intracranial CED developed antibodies after treatment with a PE38-based TT[88]. Of course, the use of DT in TTs also induces immune responses. In a clinical trial with a DT-based TT designed against T and B cell malignancies, 32% of patients had anti-DT antibodies before treatment and 100% of patients were immunogenic after only one treatment cycle. The future success of TTs depends largely on techniques, such as that of Onda and Pastan described above, to "deimmunize" biologicals in order to allow sustained treatment[86].

Materials and Methods

1. Construction of targeted toxins

Synthesis and assembly of hybrid genes encoding the single-chain DTEGFATF and EGFATFKDEL were accomplished previously in our lab using DNA-shuffling and DNA cloning techniques. The fully assembled fusion gene (from 5' end to 3' end) consisted of an *Nco*I restriction site, an ATG initiation codon, the genes for human EGF, the downstream 135-amino terminal fragment (ATF) from urokinase linked by a 20 amino acid segment of human muscle aldolase (HMA), the 7 amino acid EASGGPE linker, the first 389 amino acids of diphtheria toxin or 362 amino acids of the pseudomonas exotoxin (with KDEL replacing the REDLK at the C-terminus in PE), and a *Not*II restriction site at the 3' end of the construct. The HMA segment was incorporated into the molecule as a flexible, non-immunogenic linker[24]. The use of the ATF gene fragment was previously described by our laboratory[13,71]. The resultant 1748 bp *Nco*I/*Not*II fragment gene was spliced into the pET28c bacteria expression vector under control of an isopropyl-b-D-thiogalactopyranoside (IPTG) inducible T7 promoter. The pET system is a widely used and well established procedure for gene expression in *Escherichia coli* developed in 1986 by Studier and Moffatt[89]. Incorporation of the viral T7 promoter under control by the lac operator allows inducible expression when viral T7 RNA polymerase is available and when IPTG is supplied in order to activate the lac operator. The vector also includes kanamycin resistance as a selectable marker to ensure it has been successfully transformed into the bacterial host. DNA sequencing analysis (Biomedical Genomics Center, University of Minnesota) was used to verify that the gene was correct in sequence and had been cloned in frame. To create an EGFATFKDEL molecule with decreased immunogenicity (Figure 1), eight amino acids representing the seven major epitopes on PE38 were mutated using the QuickChange Site-Directed Mutagenesis Kit (Stratagene. La Jolla CA)[85]. The following amino acids were altered: R490A, R513A, R467A, E548S, K590S, R432G, Q332S, R313A and confirmed by DNA sequencing. Genes for monospecific targeted toxins splicing PE38KDEL to human EGF (EGFKDEL) and mutated uPA fragment (ATFKDEL) were created using the same

techniques. To demonstrate the specificity of our TTs, three negative control TTs were also produced. DTCD3CD3 (BIC3) and CD3CD3KDEL, bispecific TTs targeting T-cell surface marker CD3 were made as described previously and by replacing the DT_{390} portion of the DTCD3CD3 molecule described previously with PE38KDEL respectively[25]. 2219ARLKDEL, a BLT which combines VH and VL regions (sFv) for anti-CD22 and anti-CD19, was produced as described previously[90].

2. Isolation of inclusion bodies, refolding, and purification

Prior to my arrival in the laboratory, each plasmid (DTEGFATF/pET28c, EGFATFKDEL/pET28c, and EGFATFKDEL 7mut/pET28c) was transformed into the *Escherichia coli* strain BL21 (DE3) (Novagen). This strain of E. coli has sequences for T7 RNA polymerase, the expression of which is under the control of a lac operator. Bacteria were grown in 600 ml Luria Broth supplemented with 100 µg/ml carbenicillin in a 2 l flask at 37°C with shaking. Expression of the hybrid gene was induced by the addition of IPTG (FisherBiotech, Fair Lawn, NJ). Two hours after induction, the bacteria were harvested by centrifugation. The cell pellets were suspended and homogenized using a polytron homogenizer. After centrifugation, the pellets were extracted with 0.3% sodium deoxycholate, 5% Triton X-100, 10% glycerin, 50mM Tris, 50mM NaCl, 5mM EDTA, pH 8.0, and washed.

Solubilization of partially purified inclusion bodies was carried out in guanidine hypochloride plus 50 mM dithierythritol in the refolding buffer to decrease protein aggregation. In addition, the purity of protein isolated from the ion exchange column was further enhanced using an FPLC and Supradex 200 size exclusion column (Sigma, Ronconcoma, NY, USA). This protocol resulted in a yield of 5–10 mg of protein per liter of culture and a final product with >95% purity.

Figure 1

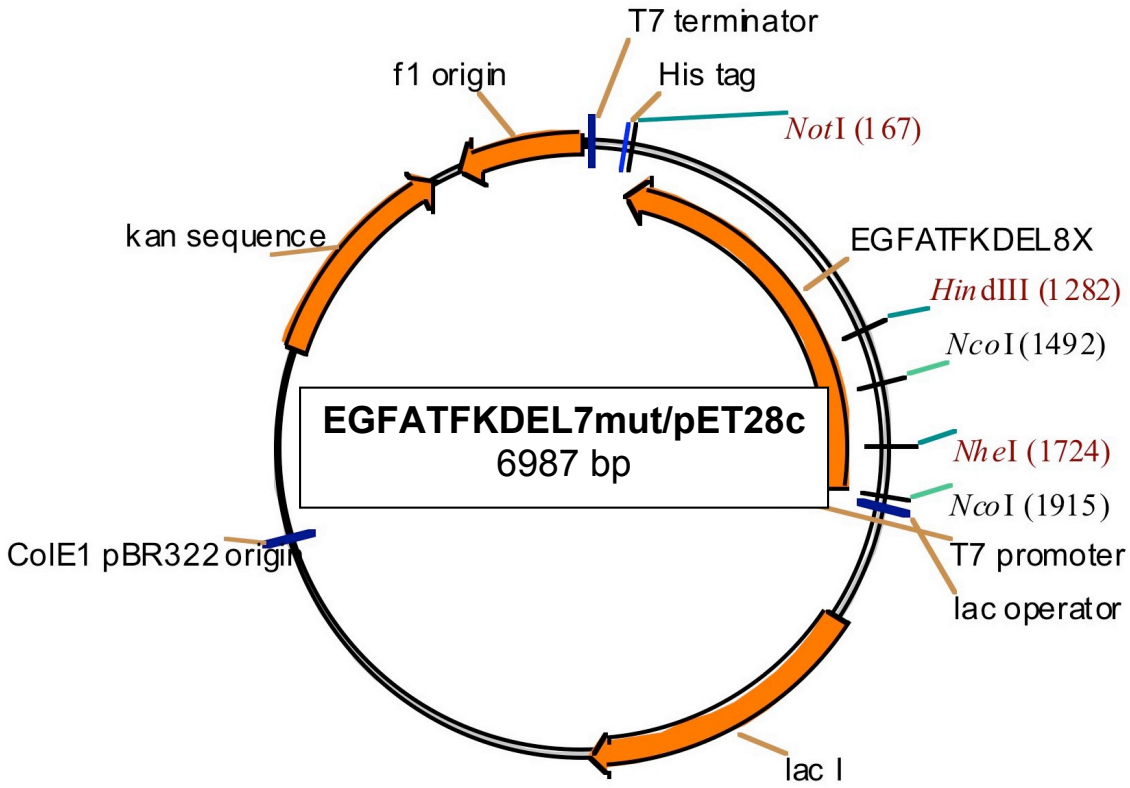

Figure 1. Gene map for EGFATFKDEL 7mut. The figure above shows the gene map for EGFATFKDEL 7mut. Maps for DTEGFATF and EGFATFKDEL were identical except for the protein coding sequence. The sequence for the catalytic portion of pseudomonas exotoxin was linked to human EGF and the amino-terminal fragment (ATF) of urokinase. The PE fragment was modified to include KDEL and remove B cell epitopes. Gene fragments from *Nco*I/*Not*I double digestion were cloned into the pET28c bacterial expression vector, which features the sequence for kanamycin resistance for selection of positively transformed clones, and a viral T7 promoter under the control of the lac operator. Expression of pET28c can thus be induced by supplementing transformed *E. coli* with IPTG. The figure was produced used Vector NTI 7 (Invitrogen, Carlsbad CA)

3. Cell culture

The human glioblastoma cell lines U87-MG (U87), U118-MG (U118), U373-MG (U373), and T98G (T98) were derived from patients with GBM and obtained from American Type Culture Collection (ATCC, Rockville MD). Human umbilical vein endothelial cells (HUVECs) were obtained from Dr. Sundaram Ramakrishnan (University of Minnesota). UMSCC-11B cells, a stage IV head and neck squamous cell carcinoma (HNSCC) derived from the larynx, were obtained from Dr. Frank Ondrey (University of Minnesota)[91]. Raji cancerous B cells, derived from human Burkitt's Lymphoma, were used as a control cell line. Cells were grown in DMEM (U87), MEM (UMSCC-11B), or RPMI-1640 media (Raji, U118, U373, and T98) supplemented with 10% fetal bovine serum, 2 mmol/l L-glutamine, 100 units/ml penicillin, and 100 μg/ml streptomycin. U87-Luc cells, which were stably transfected with vectors containing both the firefly luciferase (Luc) and blastocidin resistance genes, were maintained in DMEM with the supplements above and blastocidin. HUVECs were maintained in Medium 199 containing epidermal cell growth media supplement (Invitrogen-Gibco, Carlsbad CA), 15% heat-inactivated fetal bovine serum, and the antibiotics listed above. All carcinoma cells were grown as monolayers and Raji cells in suspension using culture flasks. Cell cultures were incubated in a humidified 37°C atmosphere containing 5% CO_2. When adherent cells were 80–90% confluent, they were passaged using trypsin-EDTA for detachment. Only cells with viability >95%, as determined by trypan blue exclusion, were used for experiments.

4. Flow cytometry analysis of EGFATFKDEL

To measure binding to U87 cells, EGFATFKDEL, EGFKDEL, ATFKDEL, RFB4 (a negative control monoclonal antibody binding to CD22 on B cells), and HD37 (a negative control monoclonal antibody binding to CD19 on B cells) were labeled with fluorescein isothiocyanate (FITC) as described previously[22,90]. FITC-labeled proteins at 500 nM were incubated with $5x10^5$ cells in 200 μl of PBS + 2% FBS on ice for 1hr to allow binding. Following incubation, cells were washed three times and binding was measured using FACSCalibur and CellQuest software (BD Biosciences, San Jose, CA).

The percent of positive cells was determined by gating control cells which were not incubated with targeted toxin.

5. Bioassays to measure cell proliferation

To determine the ability for TTs to inhibit cells *in vitro*, proliferation assays measuring ^{3}H-thymidine incorporation were used[92]. DTCD3CD3 and CD3CD3KDEL, DT- and PE-containing molecules respectively, which target CD3 on T cells, were often used as a negative control. Briefly, cells (10^4/well) were plated out in a 96-well flat-bottomed plate and incubated overnight at 37°C with 5% CO_2. The next day, targeted toxins at varying concentrations were added to wells in triplicate. Raji cells (10^4/well) were plated and targeted toxins were immediately added at varying concentrations. Plates were incubated at 37°C and 5% CO_2 for 72 h. [Methyl-^{3}H]-thymidine (GE Healthcare, UK) was added (1 μCi per well) for the final 8 h of incubation. Plates were frozen to detach cells and cells were harvested onto a glass fiber filter, washed, dried, and counted using standard scintillation methods. Background counts in untreated wells ranged from <10 cpm to 500 cpm. Data from proliferation assays are reported as percentage of control counts.

In some cell lines, protein synthesis inhibition assays measuring the incorporation of radioactive leucine were used. Cells (10^4/well) were plated out in a 96-well flat-bottomed plate and incubated overnight at 37°C with 5% CO_2. The next day, existing media was aspirated and targeted toxins diluted in leucine-free medium to varying concentrations were added to wells in triplicate. Plates were incubated at 37°C and 5% CO_2 for 72 h. [Methyl-^{3}H]-leucine (GE Healthcare, UK) was added (1 μCi per well) for the final 24 h of incubation. Plates were frozen to detach cells and cells were harvested onto a glass fiber filter, washed, dried, and counted using standard scintillation methods. Background counts in untreated wells ranged from <10 cpm to 500 cpm. Data from protein synthesis inhibition assays are reported as percentage of control counts. Results from bioassays were always reproduced.

Blocking studies were conducted to test the specificity of DTEGFATF and EGFATFKDEL 7mut. Briefly, EGF, EGFATF, or anti-uPA (American Diagnostica,

Stamford CT) was added to the media containing 0.1 nM DTEGFATF or EGFATFKDEL 7mut at a final concentration of 100 nM. Anti-diphtheria toxin and anti-pseudomonas exotoxin A (Sigma-Aldrich, St. Louis MO) were obtained as whole rabbit serum and added to medium to reach a final dilution of 1:10,000. Resulting mixtures were added to wells containing U87 cells and proliferation was measured as described above. The mouse leukocyte specific antibody anti-Ly5.2 was included as a negative control[93].

6. Determining immunogenicity of deimmunized EGFATFKDEL 7mut in mice

Mouse immunization studies were used to determine whether mutated EGFATFKDEL 7mut elicited less of an immune response than the unmutated parental EGFATFKDEL molecule. Female BALB/c or C57BL/6 mice (n=5/group) were injected intraperitoneally once weekly with 0.25 μg of either EGFATFKDEL or EGFATFKDEL 7mut for 104 days. Each week, five days after injection, the mice were bled (via facial vein collection) to obtain serum. Serum from each mouse was isolated using centrifugation and frozen. The amount of anti-PE38KDEL IgG in each serum sample was measured using indirect ELISA. Briefly, 5 mg of purified recombinant PE38KDEL was added to each well of a 96-well microtiter plate and adhered overnight at 4°C. Unbound protein was washed away with PBS-T and blocking was performed for 1 h with 5% milk/PBS-T. Serum samples were diluted in 1:10,000 and 100 μl of each was added to appropriate wells in triplicate. Following 3 h incubation, each well was washed 3 times with PBS-T. Peroxidase-conjugated rabbit anti-mouse IgG (Sigma) was added to each well for a 2 h room temperature incubation. After washing, o-Phenylenediamine dihydrochloride substrate was added to each well. After 30 min, the absorbance at 490 nm was measured using a microplate reader. Quantification of actual anti-PE38KDEL IgG present in each sample was determined by comparing the absorbance values in each well to a standard curve prepared using M40-1 monoclonal anti-PE38KDEL antibody from Dr. Robert Kreitman (NIH, Bethesda, MD).

7. Maximum tolerated dose of EGFATFKDEL and monospecifics

To determine the maximum tolerated dose (MTD) of EGFATFKDEL, EGFKDEL, ATFKDEL, and a mixture of the two monospecifics, BALB/c mice were injected intraperitoneally three times every other day. TTs were given at amounts varying from 4-0.5 μg. Body weights were maintained every other day, and the number of deaths in all groups were recorded.

8. *In vivo* efficacy studies of EGFATFKDEL 7mut against U-87 flank tumors

Male nu/nu mice were purchased from the National Cancer Institute, Frederick Cancer Research and Development Center, Animal Production Area and housed in an Association for Assessment and Accreditation of Laboratory Animal Care-accredited specific pathogen-free facility under the care of the Department of Research Animal Resources, University of Minnesota. Animal research protocols were approved by the University of Minnesota Institutional Animal Care and Use Committee. All animals were housed in microisolator cages to minimize the potential of contaminating virus transmission.

For flank tumor studies, mice were injected with 3 x 10^6 U87-Luc cells. Once tumors reached approximately 0.075 cm^3 (day 12) or 0.03 cm^3 (day 6), mice were divided into groups and treated with EGFATFKDEL 7mut, ATFKDEL or 2219ARLKDEL. Mice in treated groups were given 2-4 μg of targeted toxin four times a week for a total of about 5-6 weeks. All targeted toxins were administered by intratumoral injection in 100 μl volume of sterile saline. Drug was delivered in this volume so that it could be injected in 3 different directions. Backflow can be a problem, especially when injecting small tumors with high intrastitial pressures. Because of the anti-angiogenic nature of our drugs, we reasoned that even if a full dose was not given entirely intratumorally, it would still affect the tissue immediately surrounding the tumor. Tumor size was measured using a digital caliper, and volume was determined as a product of length, width, and height. Treatment-related toxicity was monitored by measuring animal weight.

Mice were imaged in real time and images were captured using Xenogen Ivis imaging system (Xenogen Corporation, Hopkington MA) and analyzed with IGOR Pro

4.09a software (WaveMetrics Inc., Portaland OR). Before imaging, mice were anaesthetized using isofluorane gas. All mice received 100 µl of a 30 mg/ml^{-1} D-luciferin aqueous solution (Gold Biotechnology, St Louis MO) as a substrate for luciferase 10 min before imaging. All images represent a 5 min exposure time and all regions of interest are expressed in units of photons/sec/cm^2/sr. About 10^5 photons/sec/cm^2/sr is the background for luciferase imaging. U87-Luc cells express firefly luciferase which bioluminesces upon binding of luciferin. Bioluminescence can then be measured using imaging tools. This system allows monitoring of TT efficacy in mice throughout and after treatment without the need to sacrifice animals.

9. Statistical analyses

All statistical analyses were performed using Prism 4 (Graphpad Software, San Diego CA). Groupwise comparisons of single data points were made by Student's *t*-tests or one-way ANOVA with Tukey's multiple comparison tests. P-values <0.05 were considered significant.

Results

1. Toxicity of DTEGFATF and EGFATFKDEL against GBM

The *in vitro* activities of DTEGFATF and EGFATFKDEL were tested using U87 and U87-Luc cells (Figure 2). U87 was chosen due to the co-overexpression of EGFR and uPAR. U87-Luc cells, which had been stably transformed with the genes for firefly luciferase and blastocidin resistance, were also used. The ability to target and kill U87 and U87-Luc was measured using proliferation and protein synthesis inhibition assays. The monospecific cytotoxins, DTEGF and EGFKDEL, which target EGFR, along with DTAT and ATFKDEL, which target uPAR, were included for comparison to their respective BLTs. DTCD3CD3 and CD3CD3KDEL, bivalent TTs targeted against CD3 T cell receptors, were selected as negative controls to ensure non-specific TTs were not able to kill CD3-negative cell lines. Testing with DTEGFATF showed that the BLT markedly inhibited U87 cells in a dose dependent fashion with an inhibitory concentration 50% (IC_{50}) value of 0.032 nM. In contrast, the monospecifics DTEGF and DTAT exhibited reduced activity with IC_{50} values of 0.145 and 0.681 nM respectively (Figure 2A). An equimolar mixture of both DTEGF and DTAT was also not as potent as the bispecific. These results were not surprising because our laboratory has shown that the activities of other bispecific targeted toxins are consistently greater than their monospecific counterparts[20,21,90]. The negative control DTCD3CD3 had no effect, confirming the specificity of DTEGFATF to $EGFR^+/uPAR^+$ GBM cells. The results from an identical DTEGFATF protein inhibition assay using U87-Luc cells were comparable, confirming that the firefly luciferase-transformed cells are biologically identical to the parental U87 cell line (Figure 2B). Testing EGFATFKDEL revealed similar results and TT activities in both U87 and U87-Luc cells (Figure 2C-D). These results indicated that our two BLTs recognize EGFR- and uPAR-expressing target cells, and that there is an advantage to using two targeting ligands to the same single chain.

Figure 2A

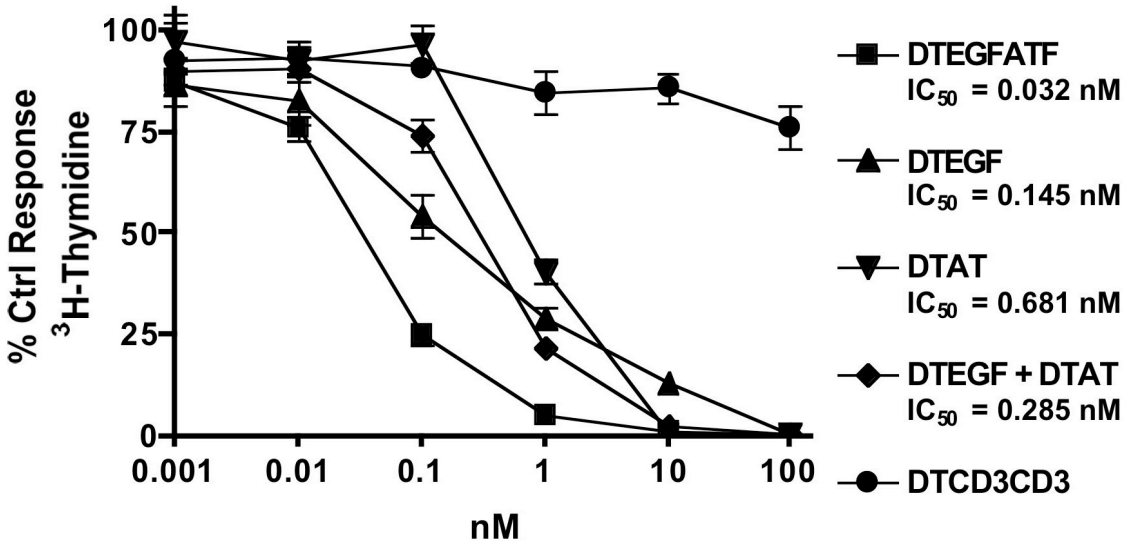

Figure 2A. Effect of DTEGFATF on EGFR$^+$/uPAR$^+$ U87 cells. DTEGFATF and corresponding monospecific TTs were tested against U87 cells in a proliferation assay. The effects of bispecific DTEGFATF, monospecific DTEGF and DTAT, and T-cell targeting DTCD3CD3 were determined by analyzing ^{3}H-thymidine uptake after a 72-hr incubation with targeted toxins. Data are reported as percent control response. Each data point represents an average of triplicate measures ± S.D.

Figure 2B

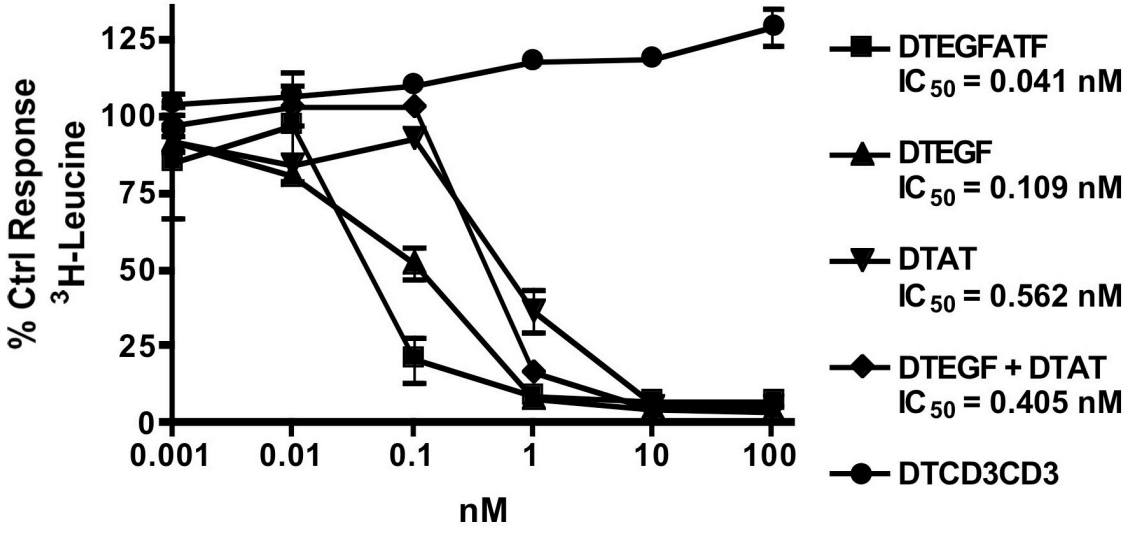

Figure 2B. Effect of DTEGFATF on U87-Luc cells. DTEGFATF and corresponding monospecific TTs were tested against U87-Luc cells in a protein synthesis inhibition assay. The effects of bispecific DTEGFATF, monospecific DTEGF and DTAT, and T-cell targeting DTCD3CD3 were determined by analyzing ^{3}H-leucine uptake after a 72-hr incubation with targeted toxins. Data are reported as percent control response. Each data point represents an average of triplicate measures ± S.D.

Figure 2C

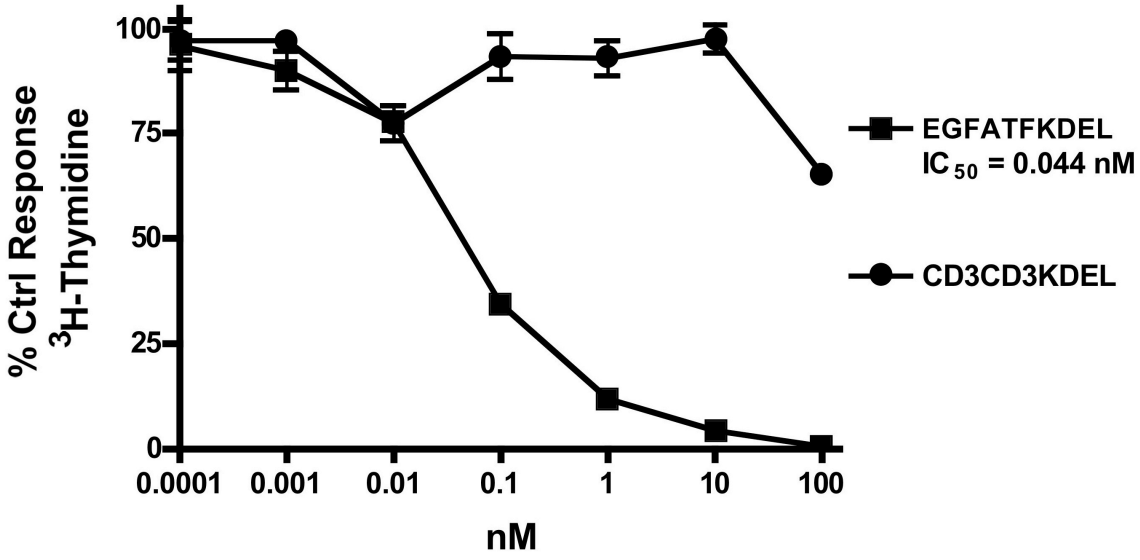

Figure 2C. Effect of EGFATFKDEL on U87 cells. EGFATFKDEL and control CD3CD3KDEL were tested against U87 cells in a proliferation assay. Effects were determined by analyzing ^{3}H-thymidine uptake after a 72-hr incubation with targeted toxins. Data are reported as percent control response. Each data point represents an average of triplicate measures ± S.D.

Figure 2D

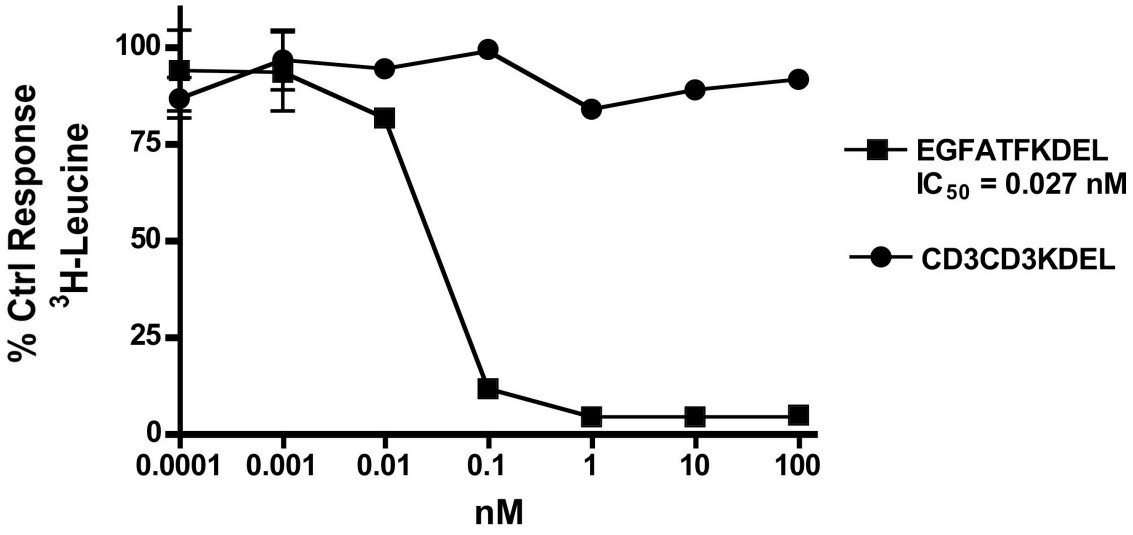

Figure 2D. Effect of EGFATFKDEL on U87-Luc cells. EGFATFKDEL and control CD3CD3KDEL were tested against U87-Luc cells in a protein synthesis inhibition assay. Effects were determined by analyzing ^{3}H-leucine uptake after a 72-hr incubation with targeted toxins. Data are reported as percent control response. Each data point represents an average of triplicate measures ± S.D.

2. Toxicity of DTEGFATF and EGFATFKDEL against endothelial cells

DTEGFATF and EGFATFKDEL are designed to target both solid GBM tumors and their associated endothelial neovasculature. The ATF portion of each respective drug, which contains the binding domain of urokinase, targets the neovasculature (and solid tumor). To investigate whether or not the uPAR-targeting ATF portion was effective, the bispecific drugs were tested on human umbilical vein endothelial cells (HUVECs) (Figure 3). These cells bear similarity to cells in the tumor neovasculature and overexpress uPAR but not EGFR. Consequently, as expected, testing with DT-containing TTs showed that HUVECs are significantly more sensitive to DTAT (IC_{50} = 0.071 nM) when compared to DTEGF (IC_{50} > 100nM) (Figure 3A). However, DTEGFATF had the highest activity with an IC_{50} of 0.004 nM. As expected, the bispecific DTEGFATF was markedly more toxic than an equimolar mixture of monospecific DTEGF and DTAT (IC_{50} = 0.466 nM). When a similar assay was run using EGFATFKDEL and its respective PE38KDEL-containing monospecifics, nearly identical results were obtained (Figure 3B). However, EGFATFKDEL (IC_{50} = 0.052 nM) was slightly less toxic than DTEGFATF. These data show further indication of an advantage of linking both ligands on the same single chain molecule.

Figure 3A

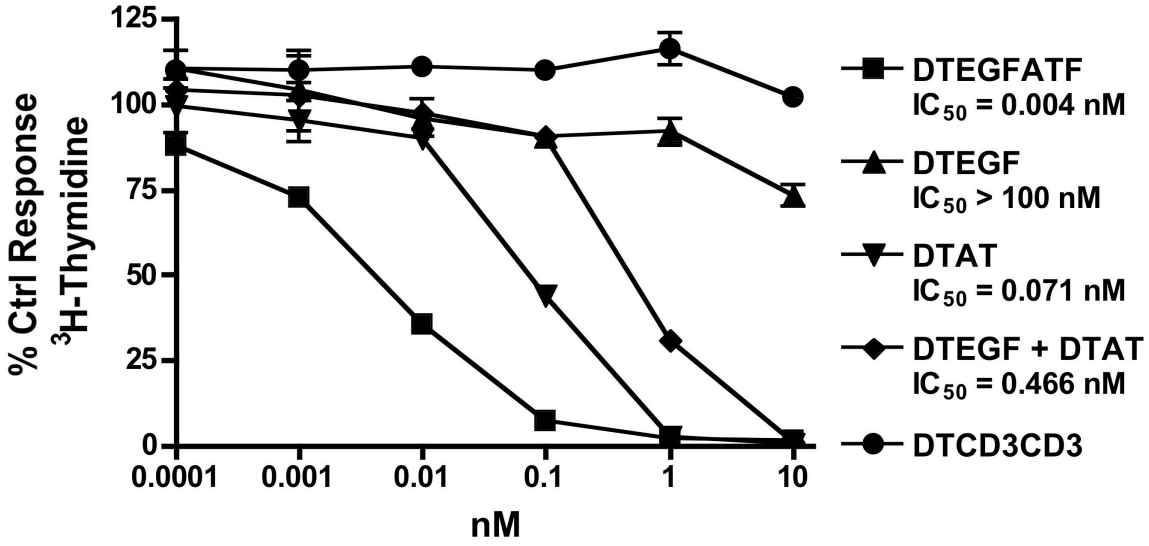

Figure 3A. Effect of DTEGFATF on HUVEC. A) The activities of DTEGFATF, DTEGF, DTAT, and DTCD3CD3 were tested against HUVEC in a ^{3}H-thymidine uptake proliferation assay to determine their ability to target tumor neovasculature.

Figure 3B

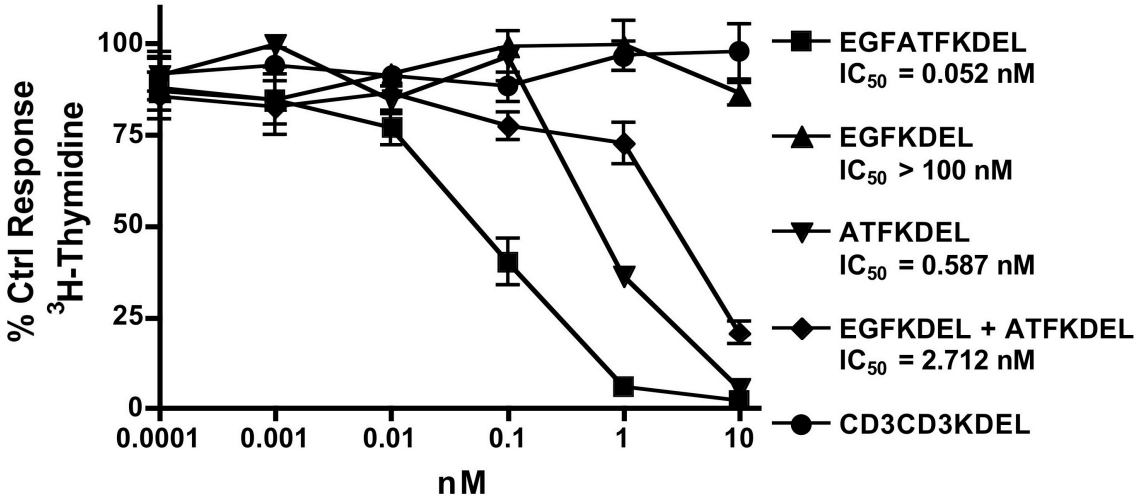

Figure 3B. Effect of EGFATFKDEL on HUVEC. Activities of PE-based EGFATFKDEL, EGFKDEL, ATFKDEL, and CD3CD3KDEL against HUVEC were measured in a ^{3}H-thymidine uptake proliferation assay.

3. Activity of EGF and ATF targeting ligands

To ensure that both high affinity cytokines, EGF and ATF, on the DTEGFATF molecule bound to their appropriate receptors, anti-urokinase antibody (α-uPA), EGF, and anti-diphtheria toxin antibody (α-DT) were incubated with a known cytotoxic concentration of DTEGFATF in attempt to block killing (Figure 4A). All of these blocking agents inhibited DTEGFATF's ability to kill U87 cells. α-DT blocked only moderately (<50%), but the remaining compounds all blocked up to 70% of the activity of DTEGFATF. In contrast, anti-Ly5.2 (α-Ly5.2), an irrelevant, murine-specific control antibody, did not block DTEGFATF activity. Additionally, a blocking assay was run using EGFATFKDEL 7mut (a BLT almost identical to EGFATFKDEL discussed later) (Figure 4B). Like the previous assay, α-uPA, EGF, and anti-pseudomonas exotoxin antibody (α-PE) were used. However, in addition, an equimolar mixture of α-uPA and EGF was used to examine whether or not this blocking strategy would be more effective. Also, EGFATF, a protein similar to EGFATFKDEL but lacking the truncated PE fragment was tested. Like the DTEGFATF assay, α-uPA and EGF were capable of reducing the effect of EGFATFKDEL 7mut by about 70%. However, the blocking agent combination and EGFATF, were able to block the effect of EGFATFKDEL at levels greater than 85%. These results confirm that both the EGF and ATF ligands are active on the DTEGFATF and EGFATFKDEL 7mut molecules.

Figure 4A

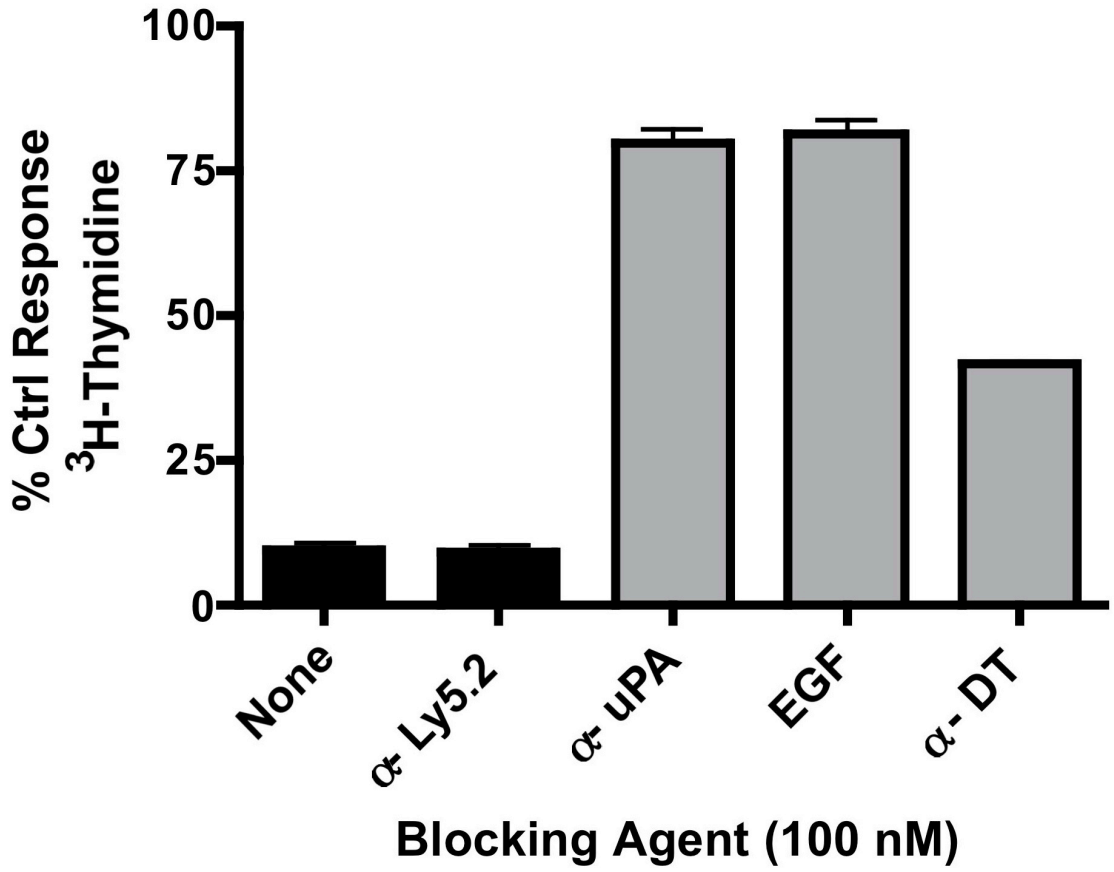

Figure 4A. Activity of both targeting ligands in DTEGFATF. A blocking assay testing the ability to reduce DTEGFATF activity was performed. U87 cells were incubated with 0.1 nM of DTEGFATF and 100 nM of recombinant anti-urokinase, EGF, anti-diphtheria toxin, or anti-Ly5.2. The non-specific recombinant anti-Ly5.2 was included as a negative control.

Figure 4B

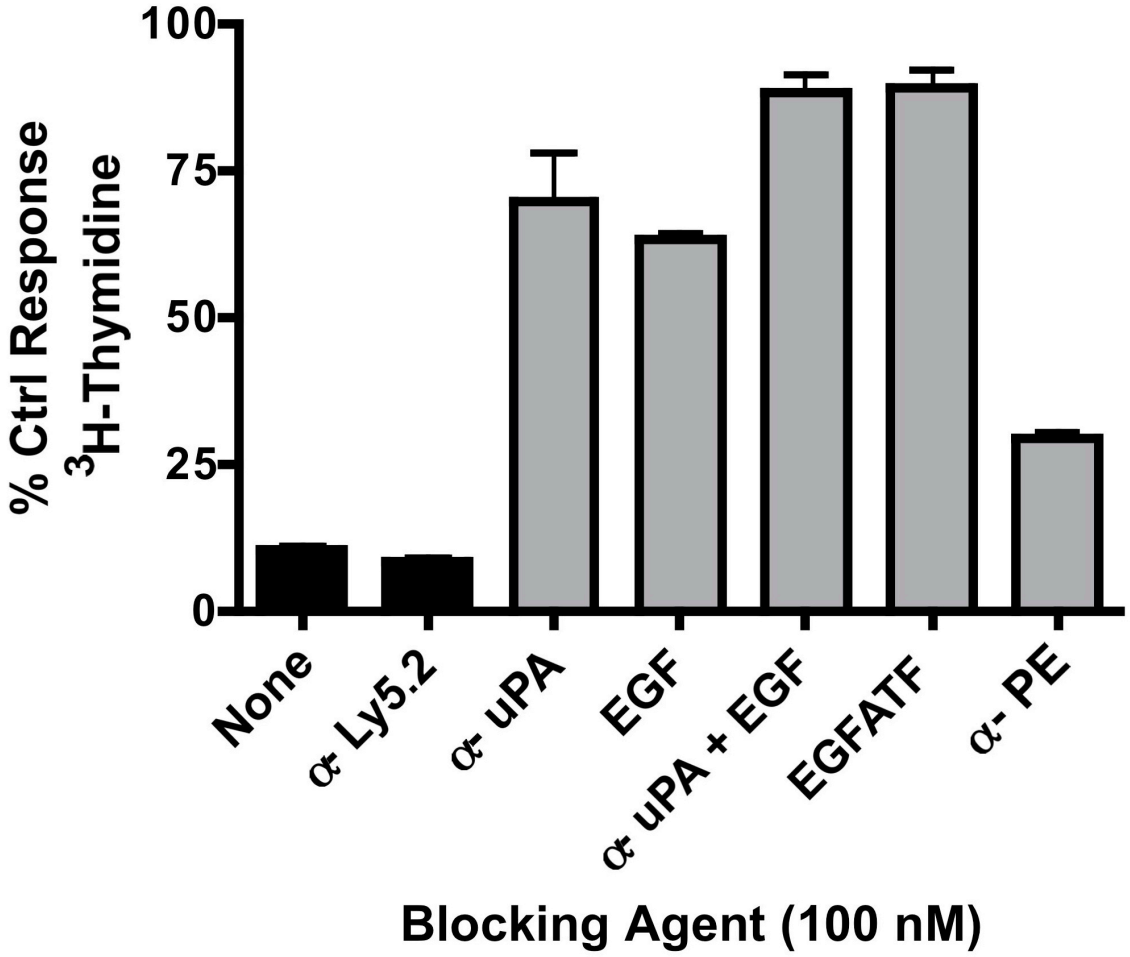

Figure 4B. Activity of both targeting ligands in EGFATFKDEL 7mut. A similar blocking assay to Figure 4A testing the ability to block EGFATFKDEL 7mut is shown using 100 nM of anti-urokinase, EGF, a mixture of the two, EGFATF, anti-pseudomonas exotoxin, and anti-Ly5.2 against 0.1 nM EGFATFKDEL 7mut.

4. Binding of EGFATFKDEL to U87 cells

The efficacy of all targeted toxins is dependent on cell surface binding and internalization. Thus, we measured ligand-mediated cell binding of EGFATFKDEL, EGFKDEL, ATFKDEL, and the negative controls HD37 and RFB4 on U87 cells (Figure 5). The binding of EGFATFKDEL was examined instead of DTEGFATF, because EGFATFKDEL was slated for further development. All of the targeted toxins were FITC-labeled, incubated with U87 cells at varying concentrations (100, 500, and 1000 nM), and analyzed using flow cytometry. At 500 nM, the percentage of positive cells was 22.8 and 34.8% with monospecific EGFKDEL-FITC and ATFKDEL-FITC, respectively. In contrast, the same cells reacted with bispecific EGFATFKDEL-FITC were 58% positive (Figure 5C). Cells stained with anti-B cell negative control HD37-FITC, bound to only 1.4% of the cells (Figure 5D). Similar findings were observed when drug concentrations were decreased to 100 nM indicating specific binding of the BLT (Figure 5A-B). At 1000nM, we observed increased binding of EGFKDEL and ATFKDEL (35.6 and 53.2% respectively), while maximum binding of EGFATFKDEL was observed (52.8%) (Figure 5E). These results suggest that the bispecific, EGFATFKDEL, exhibits increased binding rates on U87 cells when compared to monospecific EGFKDEL and ATFKDEL.

Figure 5

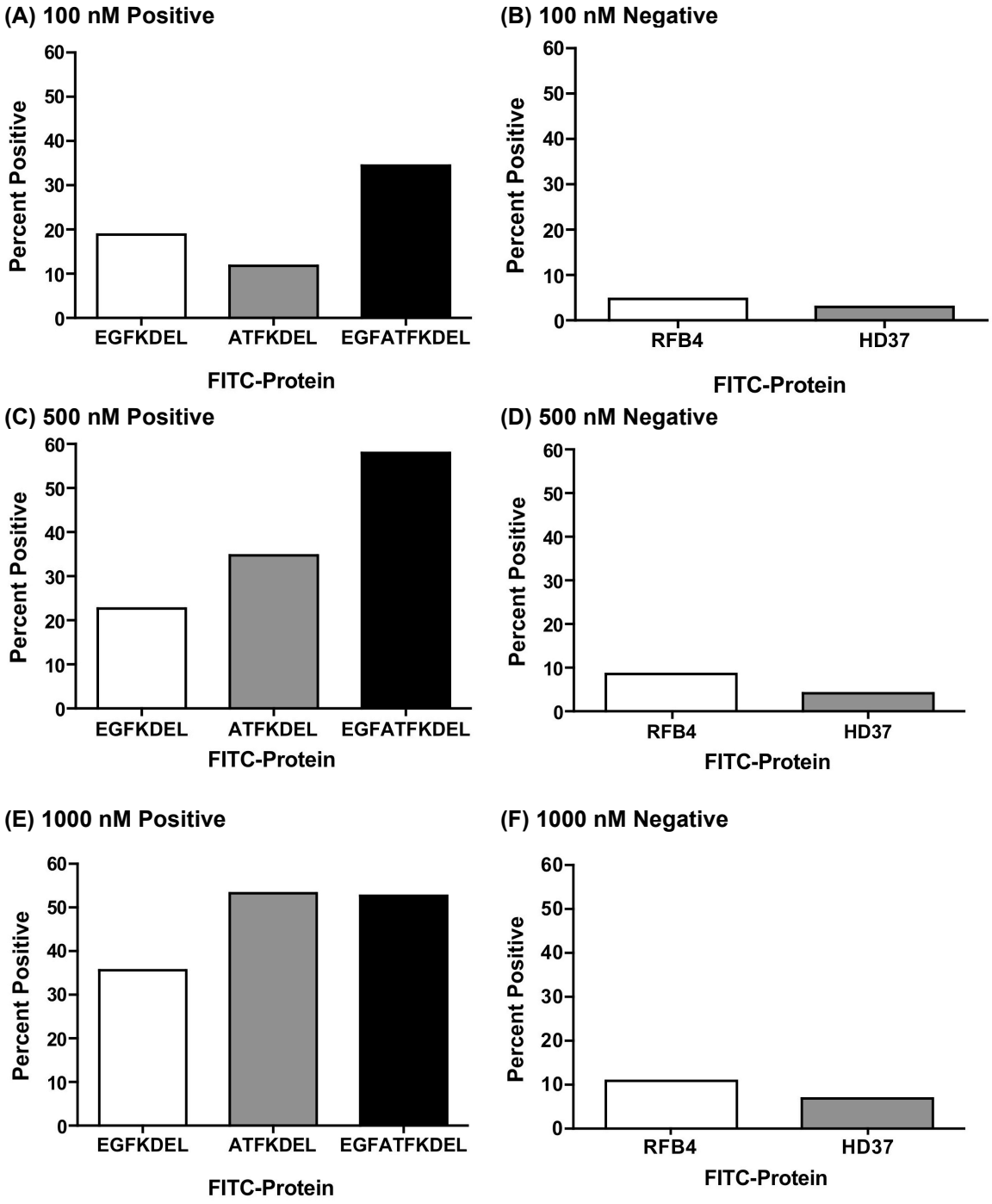

Figure 5. The ability for EGFKDEL, ATFKDEL, and EGFATFKDEL to bind to U87 cells. Percent positive values from flow cytometry analysis are graphed for U87 cells incubated in 100 nM (A-B), 500 nM (C-D), or 1000 nM (E-F) of EGFKDEL, ATFKDEL, EGFATFKDEL, RFB4, or HD37.

5. Reducing the immunogenicity of EGFATFKDEL

The efficacy of TTs and other biologicals in the treatment of solid tumors has been impaired by problems with immunogenicity[87]. Use of targeted toxins requires multiple treatments which results in the generation of antibodies that are mainly produced against the toxin portion of the drug[85,88]. Onda and Pastan recently mapped seven major immunodominant epitopes in PE that can be mutated without loss of catalytic activity[85]. By mutating eight amino acids on our PE-based BLT, we combined advancement in toxin "deimmunization" with our observation of enhanced BLT activity to produce a new anti-cancer biological drug called EGFATFKDEL 7mut.

To verify that the mutated EGFATFKDEL retained activity, the mutated and non-mutated drugs were compared *in vitro* against the U87 and U87-Luc cell lines. Mutated EGFATFKDEL 7mut consistently had significantly greater activity than parental EGFATFKDEL. Figure 6A shows the IC_{50} of EGFATFKDEL 7mut as 0.007 nM and the IC_{50} of EGFATFKDEL as 0.044 nM. Nearly identical results were found when comparing the parental and mutant BLTs in U87-Luc cells (Figure 6B). A slight increase in toxicity was also observed in HUVEC cells where the IC_{50} of EGFATFKDEL 7mut was 0.015 nM compared to 0.052 nM in the parental EGFATFKDEL (Figure 6C). To ensure that the mutations did not confer a loss of specificity, a BLT called EGF4KDEL 7mut was used. EGF4KDEL 7mut links EGF and interleukin 4 (IL-4) to PE38KDEL 7mut. The toxin portion is identical to the mutated PE fragment in EGFATFKDEL 7mut. As expected, EGF4KDEL 7mut had little ability to target the EGF-negative HUVECs. The negative control, CD3CD3KDEL was not toxic in U87, U87-Luc and HUVEC *in vitro* assays. The discrepancy in activity between EGFATFKDEL and EGFATFKDEL 7mut is peculiar. Similar increases in activity have been observed in other mutant PE38KDEL-containing drug studies but the cause is unknown[86].

To further demonstrate the specificity of EGFATFKDEL and mutant EGFATFKDEL 7mut, the TTs were incubated with $EGFR^-/uPAR^-$ Raji B cells (Figure 6D). Raji cells were not affected by EGFATFKDEL, EGFKDEL, or ATFKDEL. In contrast, 2219ARLKDEL, a bispecific toxin targeting both CD22 and CD19 expressed on Raji cells, killed the cells as anticipated (IC_{50} = 0.015 nM)[90]. The Raji protein inhibition

assay shows that EGFATFKDEL's targeting of EGFR and uPAR is specific and suggests that the probability for non-specific cross-reactivity is minimal.

Figure 6A

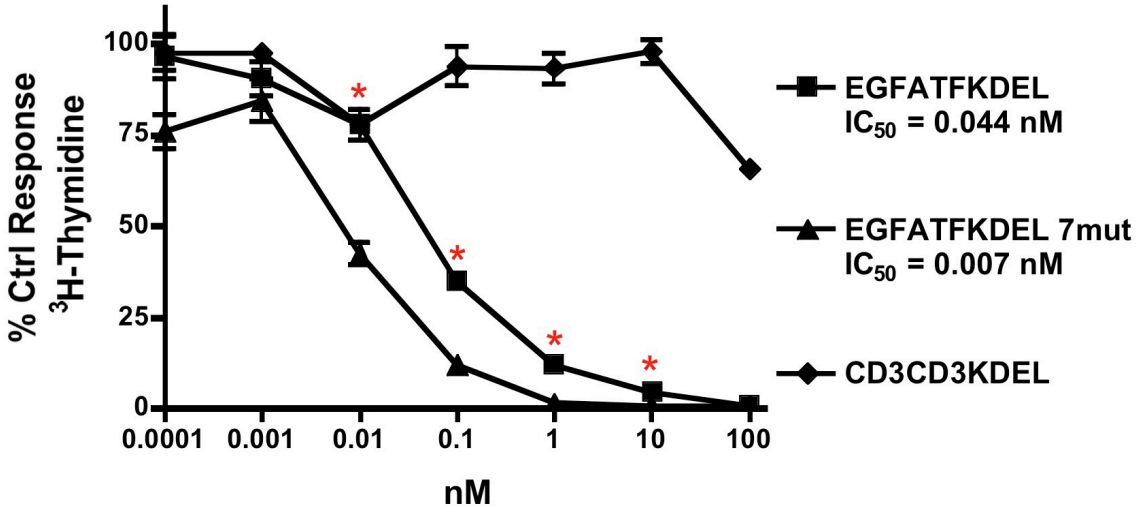

Figure 6A. Activity of deimmunized EGFATFKDEL 7mut. Mutated EGFATFKDEL 7mut was compared to unmutated parental EGFATFKDEL against U87 cells in a proliferation assay. ^{3}H-thymidine incorporation was measured after 72-hr incubation with TTs. Data are reported as percentage of control response and measurements were made in triplicates ± S.D. CD3CD3KDEL was a negative control. Significant differences between the EGFATFKDEL and EGFATFKDEL 7mut are indicated by asterisks ($p<0.05$).

Figure 6B

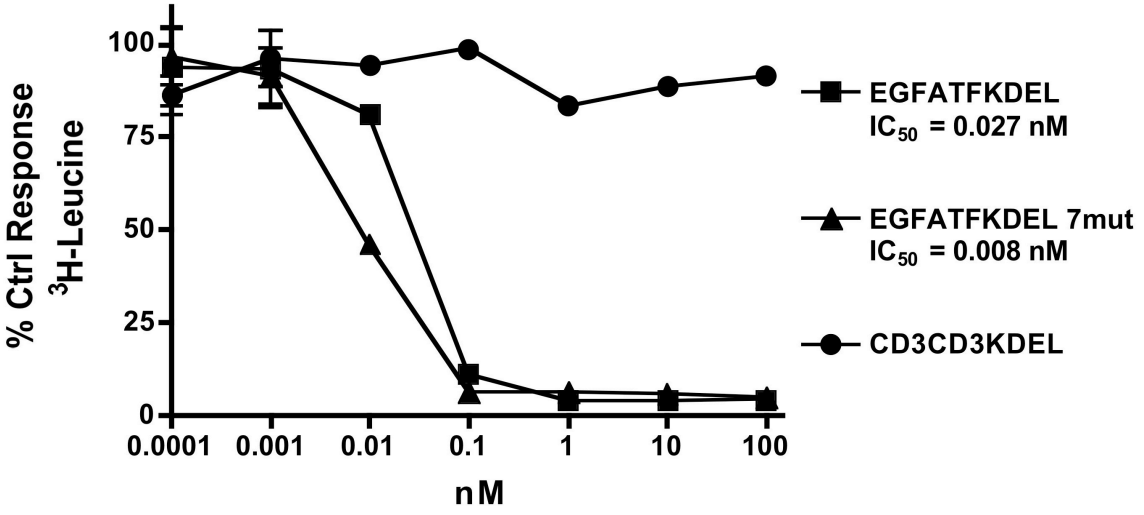

Figure 6B. Activity of EGFATFKDEL 7mut in U87-Luc cells. A protein synthesis inhibition assay was used to confirm EGFATFKDEL 7mut's activity in U87-Luc cells. CD3CD3KDEL was used as a negative control.

Figure 6C

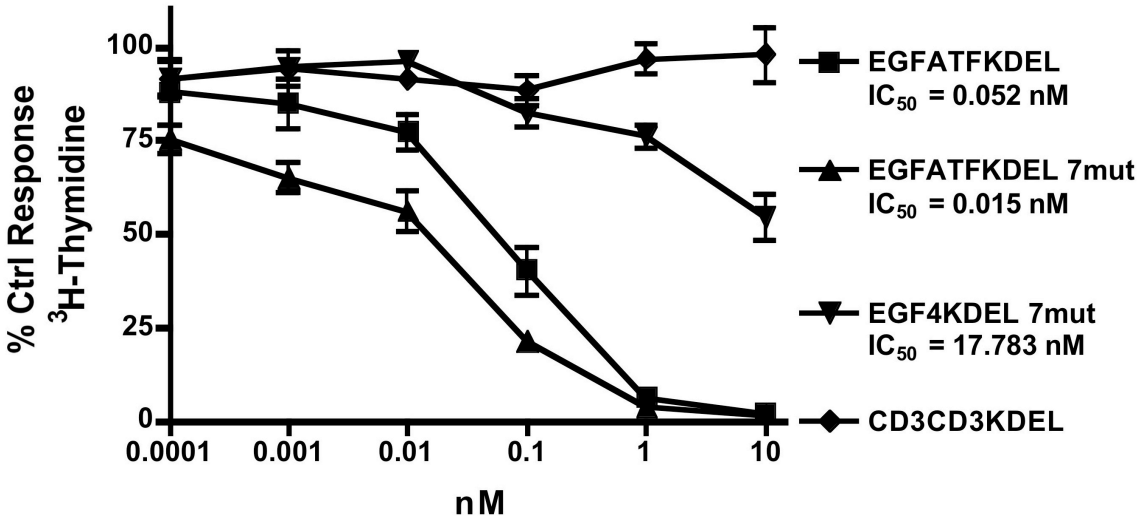

Figure 6C. Effect of EGFATFKDEL 7mut on HUVEC. The ability for the mutant BLT to target endothelial HUVECs was tested using a proliferation assay. EGFATFKDEL and EGFATFKDEL 7mut were compared to two controls. The first control, EGF4KDEL 7mut, is an EGF- and IL-4-targeting mutant BLT. The second control was CD3CD3KDEL.

Figure 6D

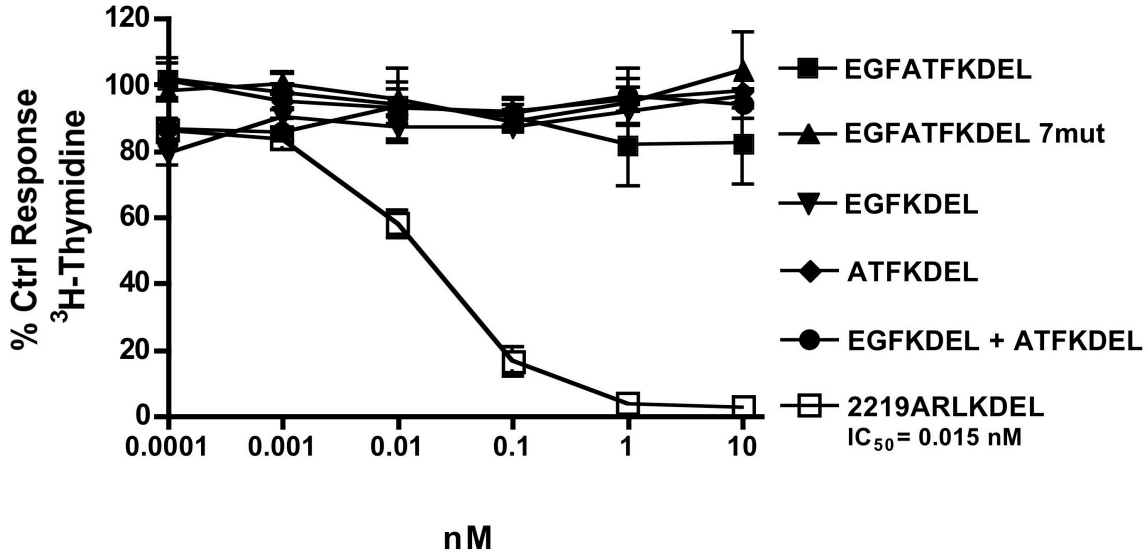

Figure 6D. Specificity of EGFATFKDEL 7mut. Specificity of EGFATFKDEL and EGFATFKDEL 7mut was shown by testing its activity toward $EGFR^{-}$/$uPAR^{-}$ Raji B cells in a proliferation assay. 2219ARLKDEL was used as a positive control.

The effect of EGFATFKDEL 7mut is shown against other human glioblastoma cell lines including U118, U373, and T98 in Table 1. The bispecific drug was effective against all of the glioblastoma cell lines tested. UMSCC-11B, a cell line from a stage IV head and neck squamous cell carcinoma (HNSCC) patient, was chosen as a non-GBM EGF-positive cell line to test the ability for EGFATFKDEL 7mut to target a variety of human cancer cell lines[91]. Similar parental versus mutant differences in activity were observed in testing of GBM and HNSCC cell lines.

Table 1: Cytotoxicity

GBM Cell Lines	**EGFATFKDEL 7mut IC_{50} (nM)**
U87	6.5×10^{-3}
U87-Luc	7.9×10^{-3}
U118	4.83×10^{-8}
U373	$<1.0 \times 10^{-8}$
T98	9.17×10^{-8}
HNSCC Cell Lines	
UMSCC-11B	3.2×10^{-5}

To determine whether EGFATFKDEL had been successfully deimmunized, groups of immunocompetent BALB/c mice were immunized weekly with 0.25 μg of either non-mutated EGFATFKDEL or mutated EGFATFKDEL 7mut. Mice were used because the same seven major epitopes are recognized in mice and humans[94].Animals were immunized intraperitoneally (i.p) over the period of 62 days. Serum samples were obtained weekly and analyzed using ELISA to detect anti-PE38KDEL IgG. The results of the immunization experiment are summarized in Figure 7 and show statistical differences between the anti-toxin responses of the two groups ($p<0.05$). After nine injections (day 62), the EGFATFKDEL 7mut group showed no immune response, while the EGFATFKDEL group had an average anti-PE38KDEL response of 5,664 μg/ml. A similar evaluation of C57BL/6 mice showed the same results (not shown).

Figure 7

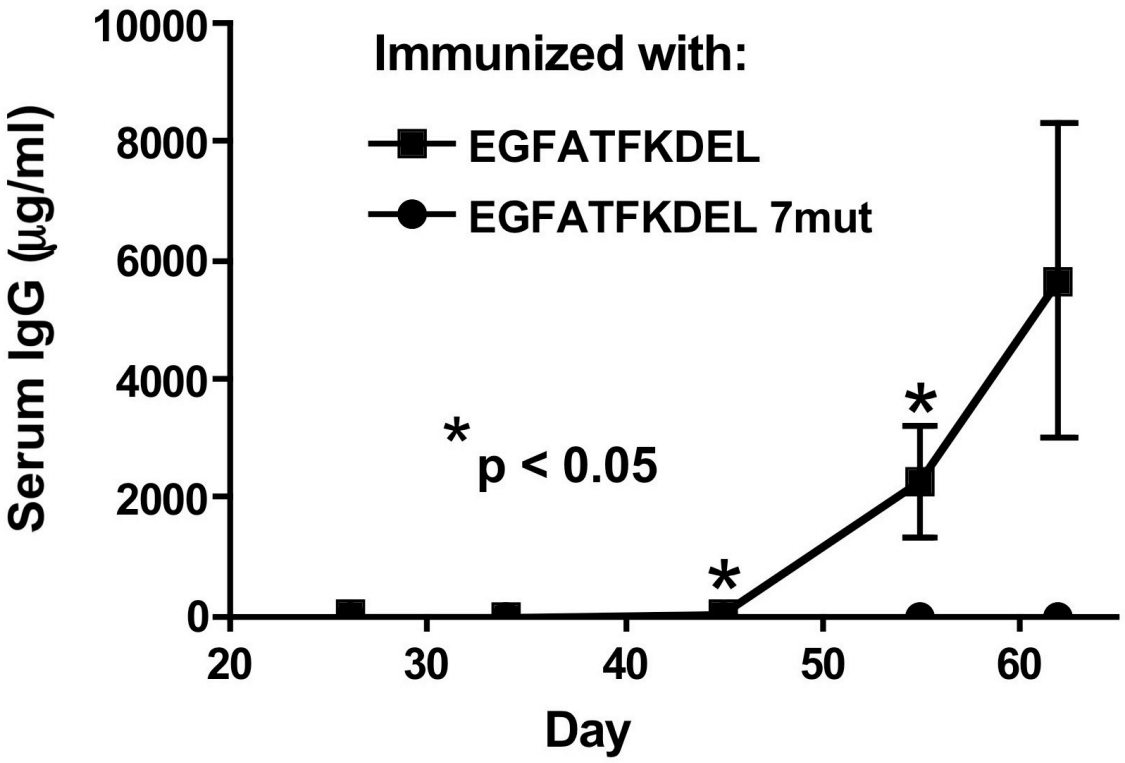

Figure 7. Immunogenicity of a mutated TT, EGFATFKDEL 7mut. The immune response to EGFATFKDEL and EGFATFKDEL 7mut was determined by measuring anti-PE38KDEL serum IgG on weekly samples of BALB/c mice treated with 0.25ug of EGFATFKDEL (n=5) or EGFATFKDEL 7mut (n=5). Measurements were made using an indirect ELISA and quantification of antibodies was determined using a standard curve generated with monoclonal anti-PE38KDEL antibody. Significant differences between the two groups are indicated by asterisks ($p<0.05$).

6. Maximum Tolerated Dose of EGFATFKDEL

After verification of EGFATFKDEL's *in vitro* activity, the toxicity of the BLT was determined in BALB/c mice to establish its potential for *in vivo* experimentation (Table 2). Toxicity testing was also conducted using monospecifics to further distinguish EGFATFKDEL's therapeutic advantages over monospecific TTs. Maximum tolerated doses (MTDs) were determined over the course of one week. Groups of mice were injected i.p with varying amounts of TT, three times, every other day. The body weights and deaths of mice were recorded after each injection. Deaths are summarized in Table 2. The toxicities of the targeted toxins varied. The monospecific, EGFKDEL and ATFKDEL, had MTDs of ~0.5 μg and ~2 μg, respectively. Accordingly, an equimolar mixture of EGFKDEL and ATFKDEL had an MTD of approximately 1 μg. EGFATFKDEL had a higher MTD (~4 μg) than either of the monospecifics alone as well as a mixture of the two monospecifics. While the MTD of EGFATFKDEL 7mut was not determined before further *in vivo* investigation was initiated, we assumed that the mutant BLT would be slightly more toxic than the parental due to results from several protein inhibition assays (Figure 6). This assumption was supported by the few deaths that occurred during treatment of tumor mice (Figure 12).

Table 2: Deaths / Total Animals

Dose (μg)	EGFATFKDEL	EGFKDEL	ATFKDEL	EGFKDEL + ATFKDEL
4.0	1 / 4	ND	ND	ND
2.0	0 / 4	4 / 4	3 / 4	ND
1.0	0 / 4	3 / 4	0 / 4	3 / 4
0.5	0 / 4	1 / 4	0 / 4	1 / 4

ND = Not Done

7. *In vivo* efficacy of EGFATFKDEL 7mut against U87-Luc flank tumors

To study the *in vivo* activity of EGFATFKDEL 7mut we used a bioluminescence luciferase reporter gene mouse model with U87-Luc cells in athymic mice. U87-Luc cells stably express firefly luciferase without affecting cell growth. This model enables real-time imaging of flank tumors. Two similar mouse experiments were run. In both experiments, athymic mice were inoculated with 50 μl of $3x10^6$ U87-Luc cells suspended in a mixture of PBS and a basement membrane matrix called matrigel. A course of treatment was defined as four consecutive daily treatments per week. Efficacy of EGFATFKDEL 7mut treatment was monitored through tumor volume, body weight, and luciferase bioluminescence measurements. Tumor volumes and body weights were taken twice per week before and after a course of treatment, whereas imaging was conducted on a weekly basis. Tumor volumes and bioluminescence consistently correlated in both experiments.

In the first experiment, when the tumors were easily palpable (Day 12; average tumor volume = 750 mm^3) the mice (n = 11) were treated with 4 μg, 3 μg, or 2 μg of EGFATFKDEL 7mut (n = 6), and the remaining mice were not treated after inoculation (n = 5) (Figures 8-10). The variability in treatment dose enabled us to determine the most efficacious dose, and mice were given six full treatment courses (day 12-50). Untreated U87-Luc tumors grew aggressively and all of the mice in this group died or were euthanized before 40 days. Treatment with EGFATFKDEL 7mut significantly inhibited tumor growth in all of the six mice, and resulted in one tumor-free mouse. However, three mice died during the course of treatment, possibly due to toxicity. Additionally, tumors did not fully regress in most mice and these tumors grew rapidly after treatment was terminated.

Figure 8A

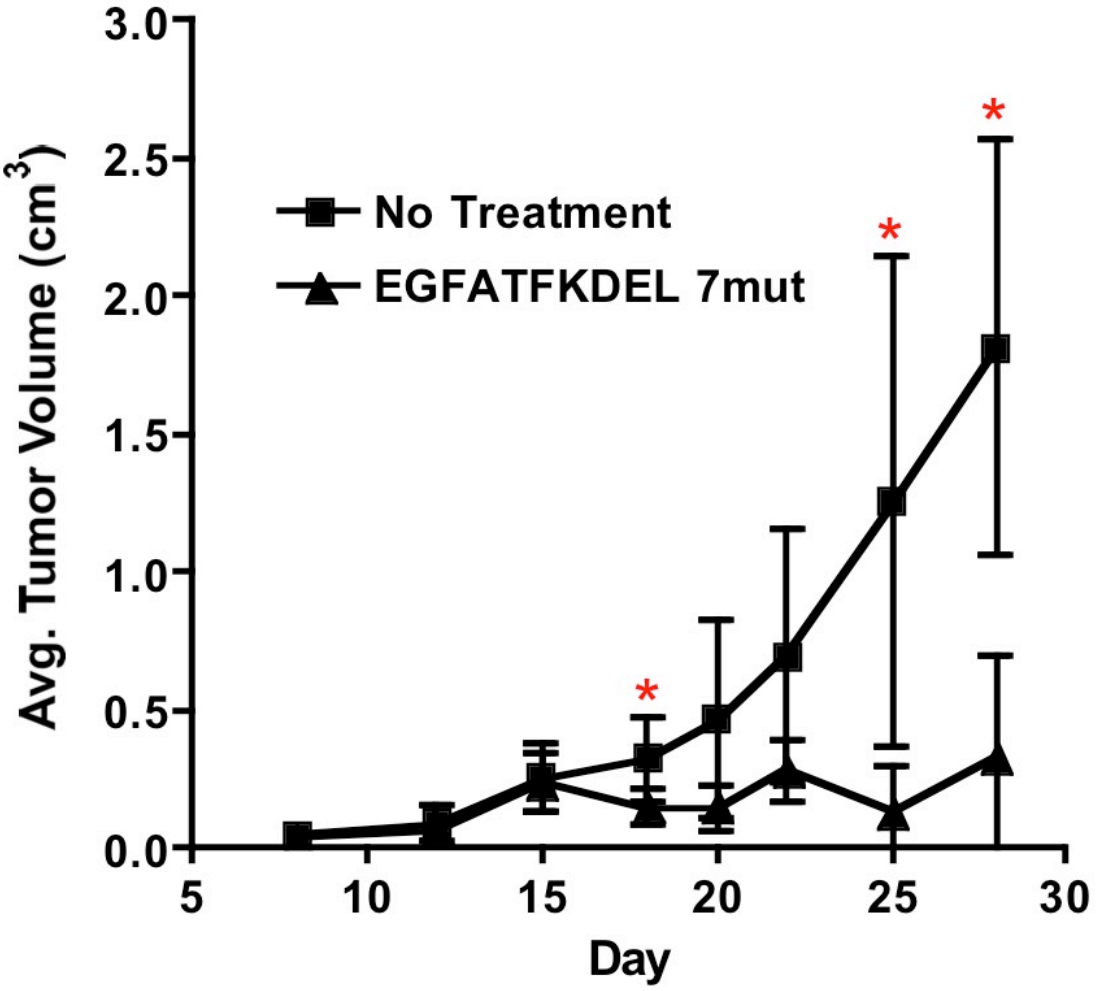

Figure 8A. Effect of intratumoral administration of EGFATFKDEL 7mut on U87-Luc flank tumor volume. Tumor volumes of mice were measured using digital calipers twice per week. Tumor volumes for both groups were averaged. Significant differences between the two groups are indicated by asterisks ($p<0.05$).

Figure 8B

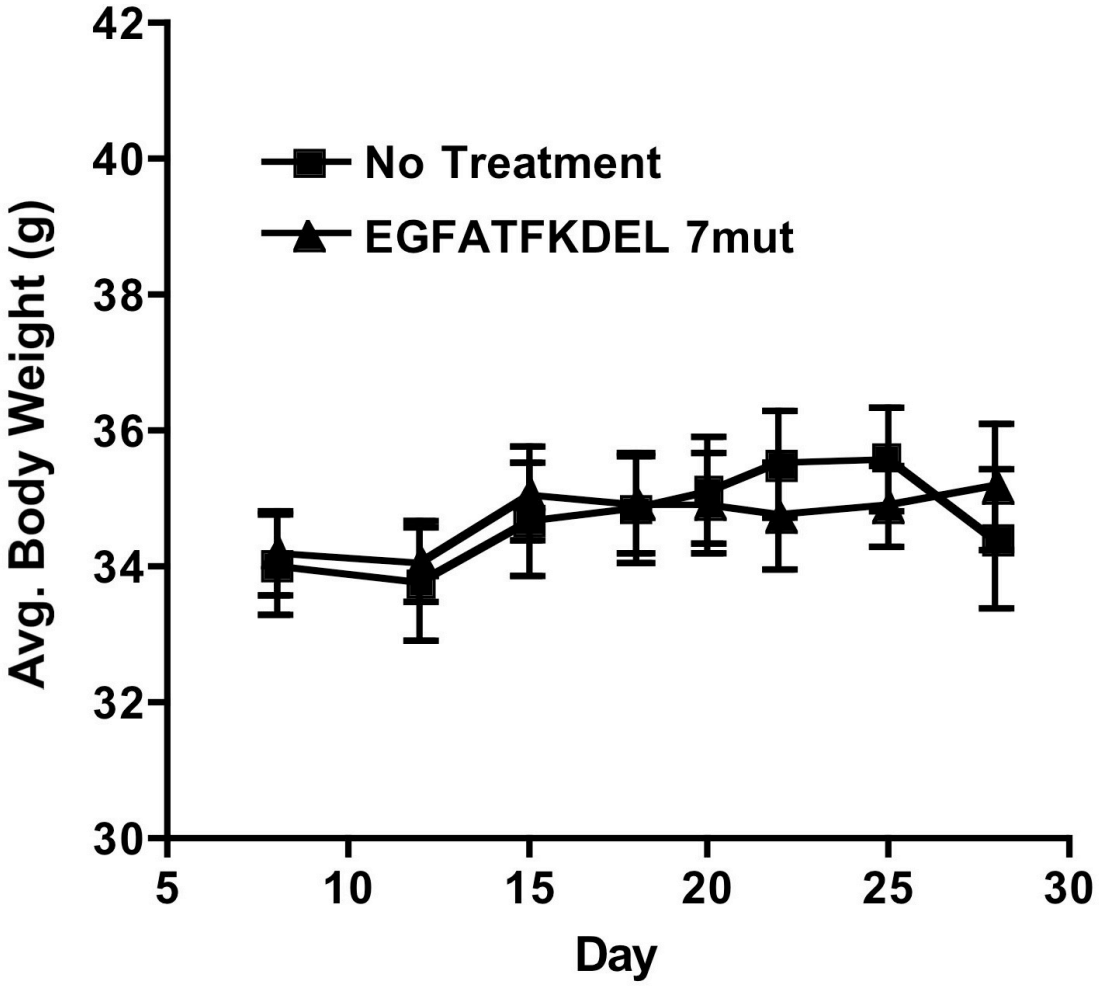

Figure 8B. Treatment associated toxicity of EGFATFKDEL 7mut administration. Body weights of mice were taken twice per week. The weights for both groups were averaged.

Figure 9A

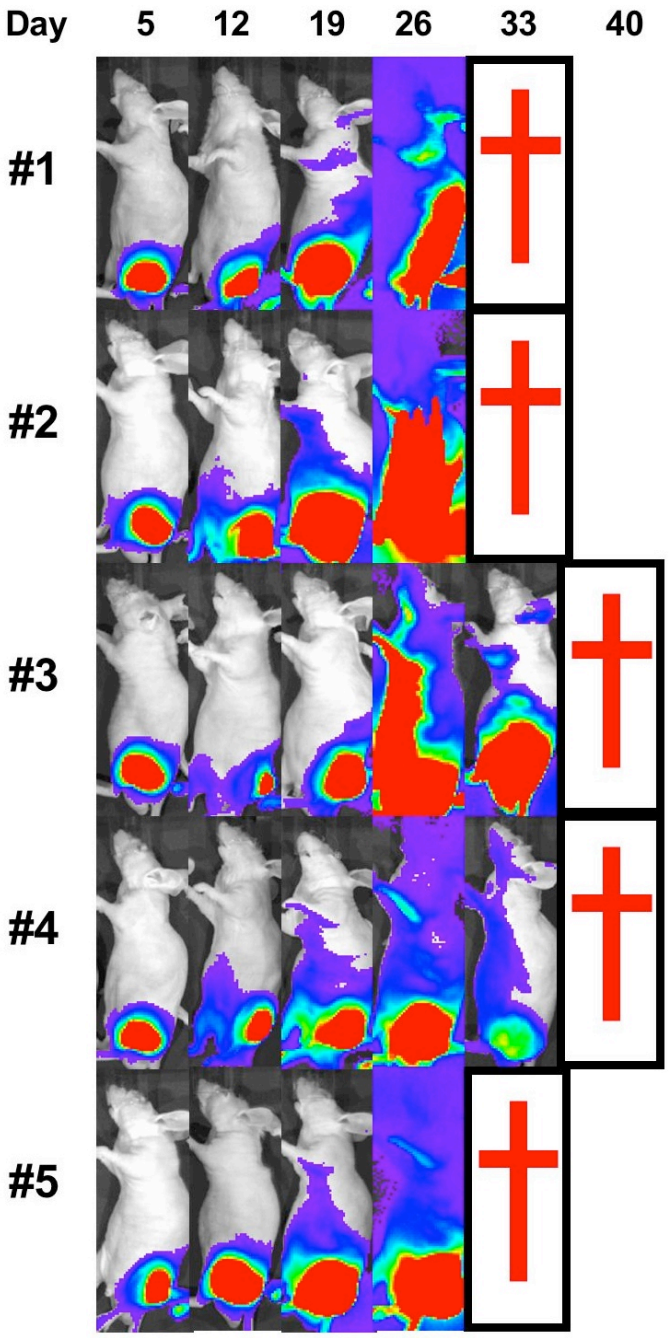

Figure 9A. Tumor growth in untreated mice. Bioluminescent images were taken of individual mice once per week. The first group was not treated after inoculation with U87-Luc cells (n=5). Crosses indicate death or euthanization.

Figure 9B

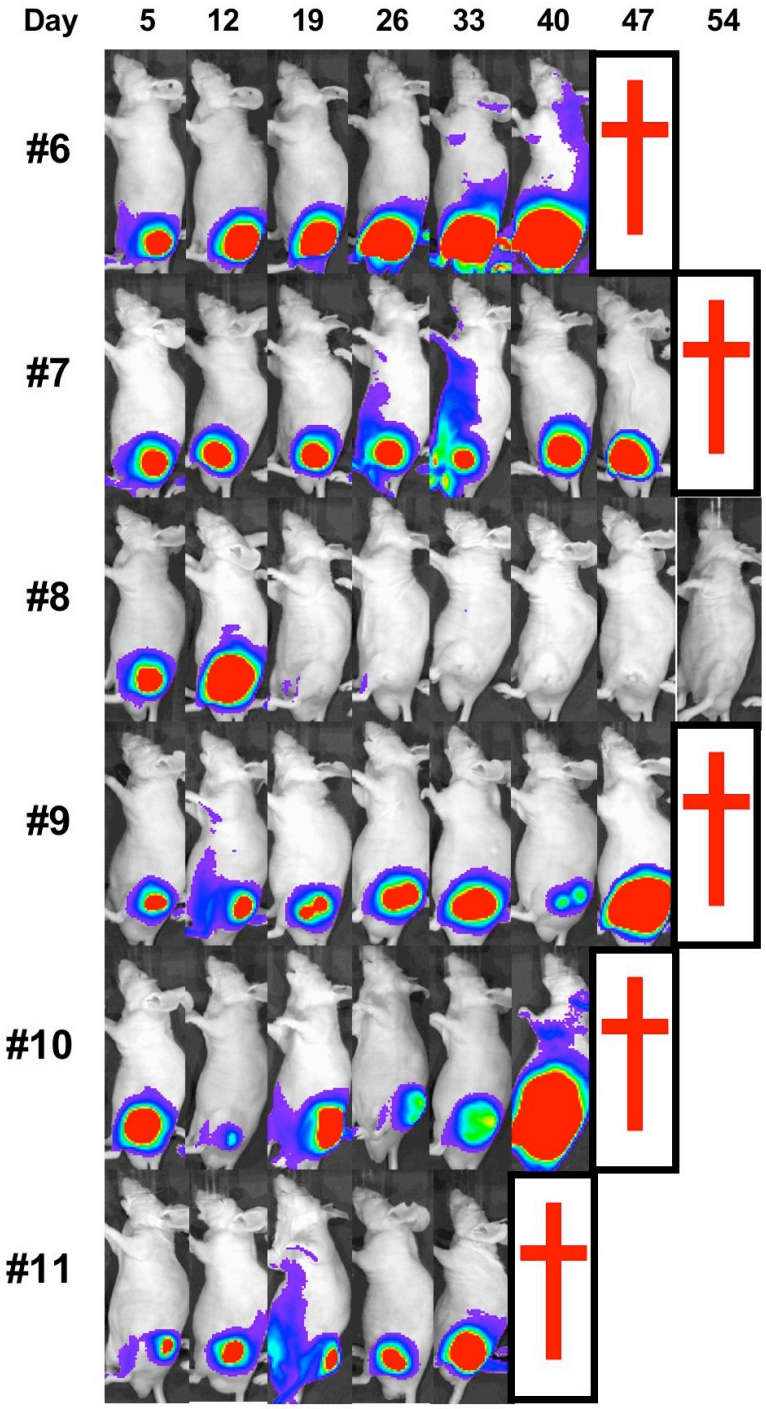

Figure 9B. Tumor regression in mice treated with EGFATFKDEL 7mut. Mice treated with EGFATFKDEL 7mut (n=6) were imaged to measure luciferase activity. Crosses indicate death or euthanization.

Figure 10A

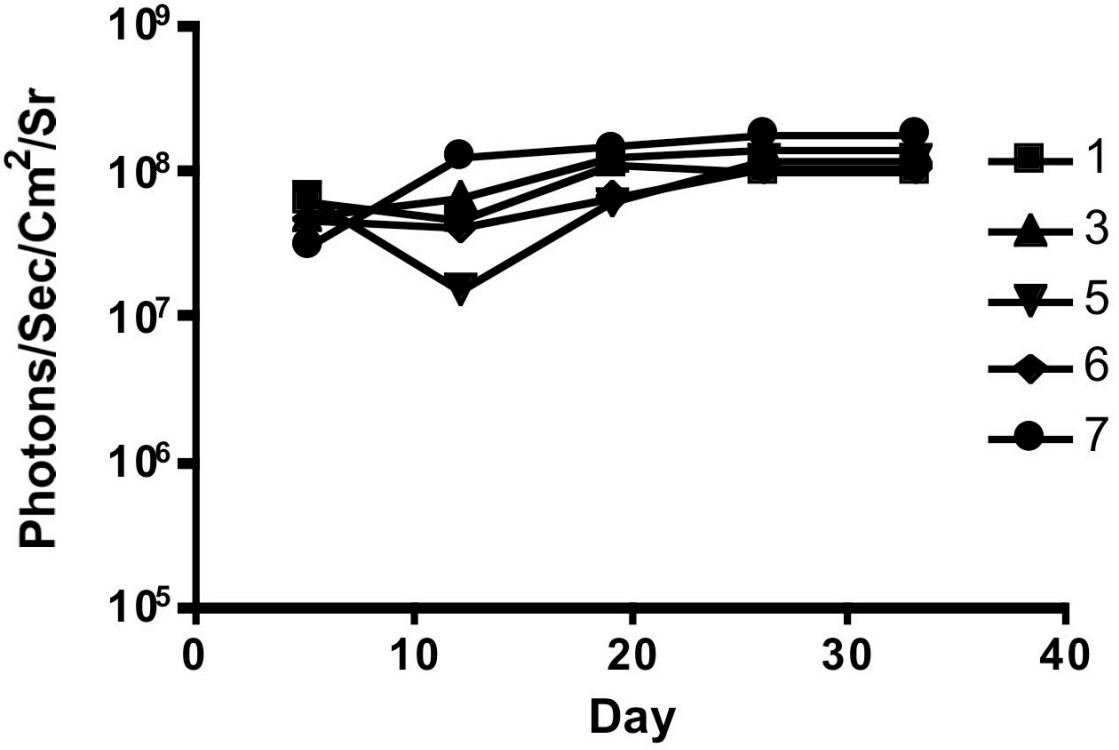

Figure 10A. Total photon tumor activity of the individual untreated mice. The amount of bioluminescence was measured during imaging of untreated mice. Bioluminescence was measured in photons/sec/cm^2/sr. The numbers represent individual mice in the treatment group.

Figure 10B

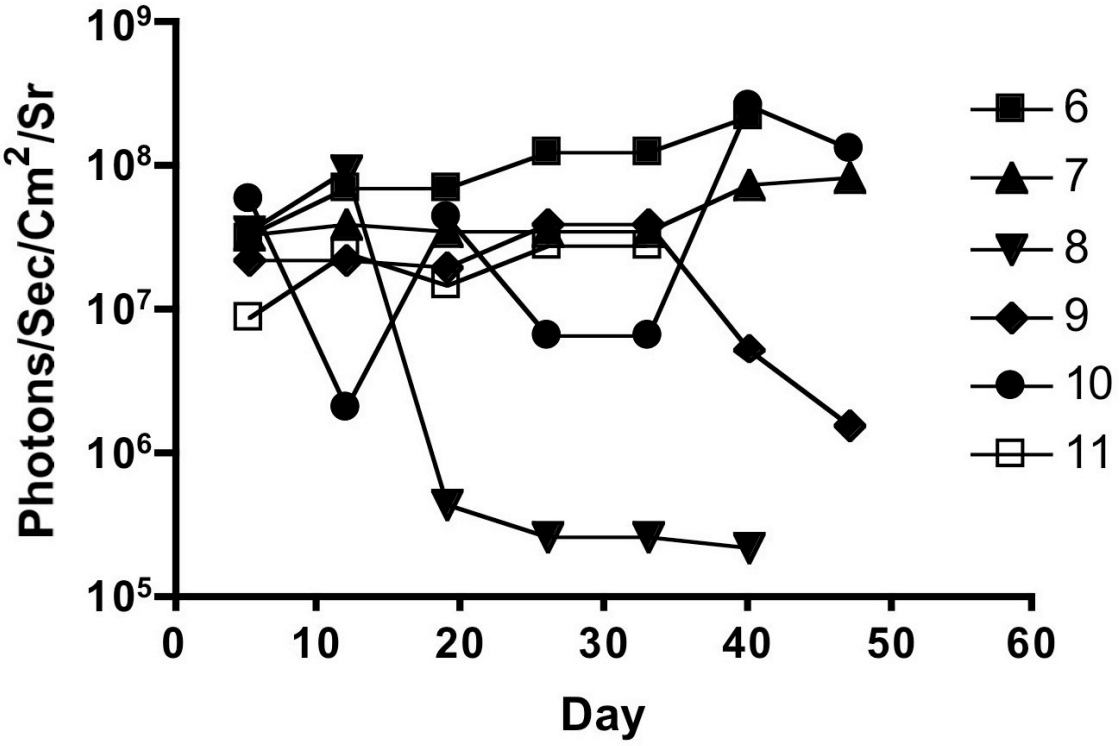

Figure 10B. Total photon tumor activity of the individual mice treated with EGFATFKDEL 7mut. Luciferase bioluminescence was measured during imaging of treatment mice throughout the course of treatment. Bioluminescence was measured in photons/sec/cm^2/sr. The numbers represent individual mice in the treatment group.

After the results of the first *in vivo* experiment were analyzed a second experiment was designed (Figures 11-13). Here, male athymic mice (n = 22) were given five courses of treatment (day 6-40) using a constant dose of 2 μg of EGFATFKDEL 7mut (n = 8), ATFKDEL (n = 5), or 2219ARLKDEL (n = 3) beginning six days after inoculation when the average tumor volume was 300 mm^3. Remaining mice were not treated after U87-Luc inoculation (n = 5). As expected, tumors in untreated mice grew aggressively until they were euthanized under regulations set by the Department of Research Animal Resources, University of Minnesota. Tumors in mice treated with the negative control, 2219ARLKDEL, grew at an almost identical rate suggesting that toxins linked to non-specific ligands cannot bind and internalize in GBM cells *in vivo*. Tumors responded well to treatment with EGFATFKDEL 7mut, and tumor volumes of mice in this group were significantly different when compared with the untreated group at days 26, 29, 33, and 36 ($p<0.05$, Figure 11A). In the long-term, even after 98 days, four out of the eight EGFATFKDEL 7mut treated mice were tumor-free. One of the tumor-free mice died on day 55 from rapid weight loss and potentially toxicity. Another tumor-free mouse died on day 99 from unknown causes.

Treatment with ATFKDEL had interesting effects. Four of the five animals treated with ATFKDEL did not elicit an anti-tumor response by day 40, but tumor volume and bioluminescence measurements remained static. These data, along with MTD analysis with EGFKDEL, indicate that the monospecific cytotoxins are not as effective as EGFATFKDEL 7mut at comparable drug concentrations

Figure 11A

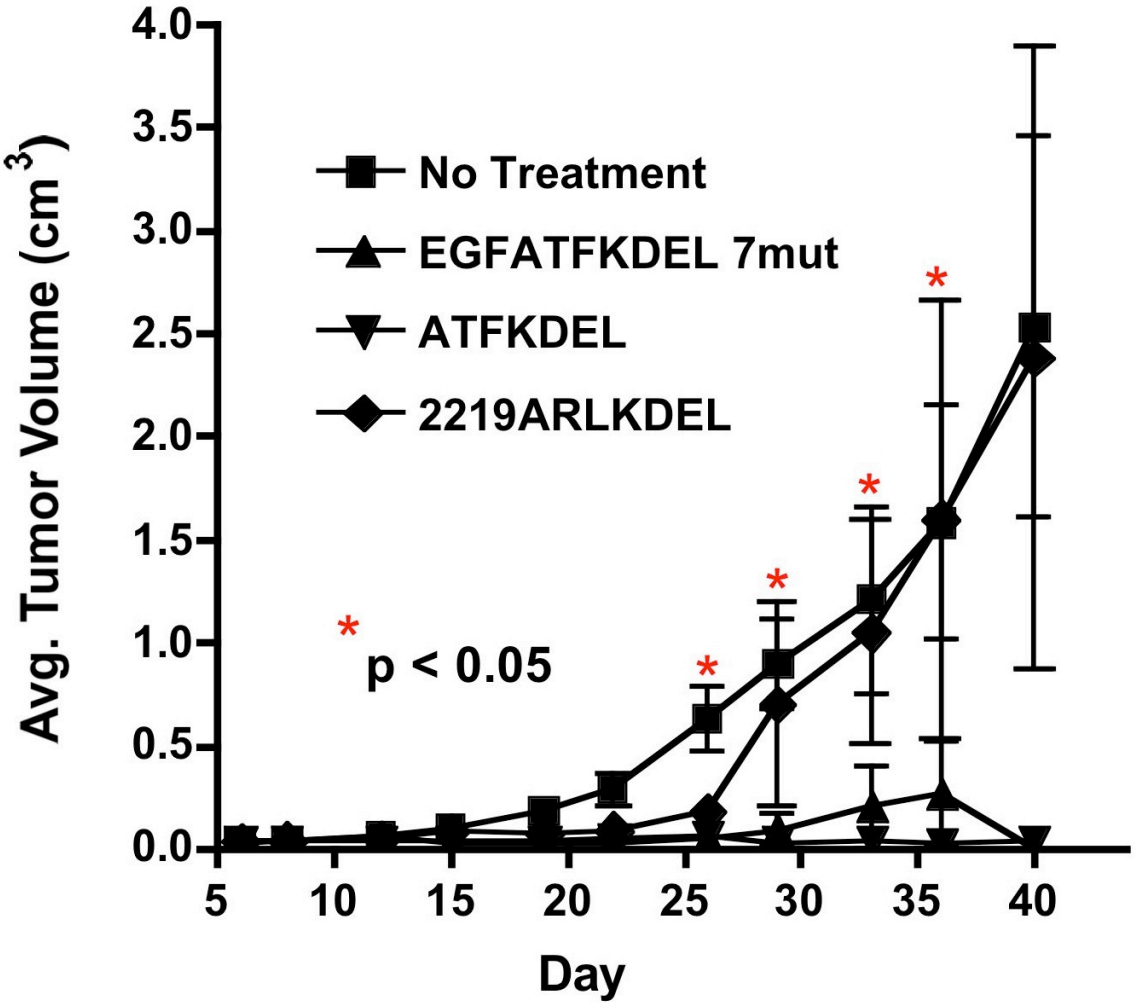

Figure 11A. Effect of intratumoral administration of EGFATFKDEL 7mut, ATFKDEL, and 2219ARLKDEL on U87-Luc flank tumor volume. Tumor volumes of mice were measured using digital calipers twice per week. Tumor volumes for each of the four groups were averaged. Significant differences between the no treatment and EGFATFKDEL 7mut groups are shown ($p<0.05$).

Figure 11B

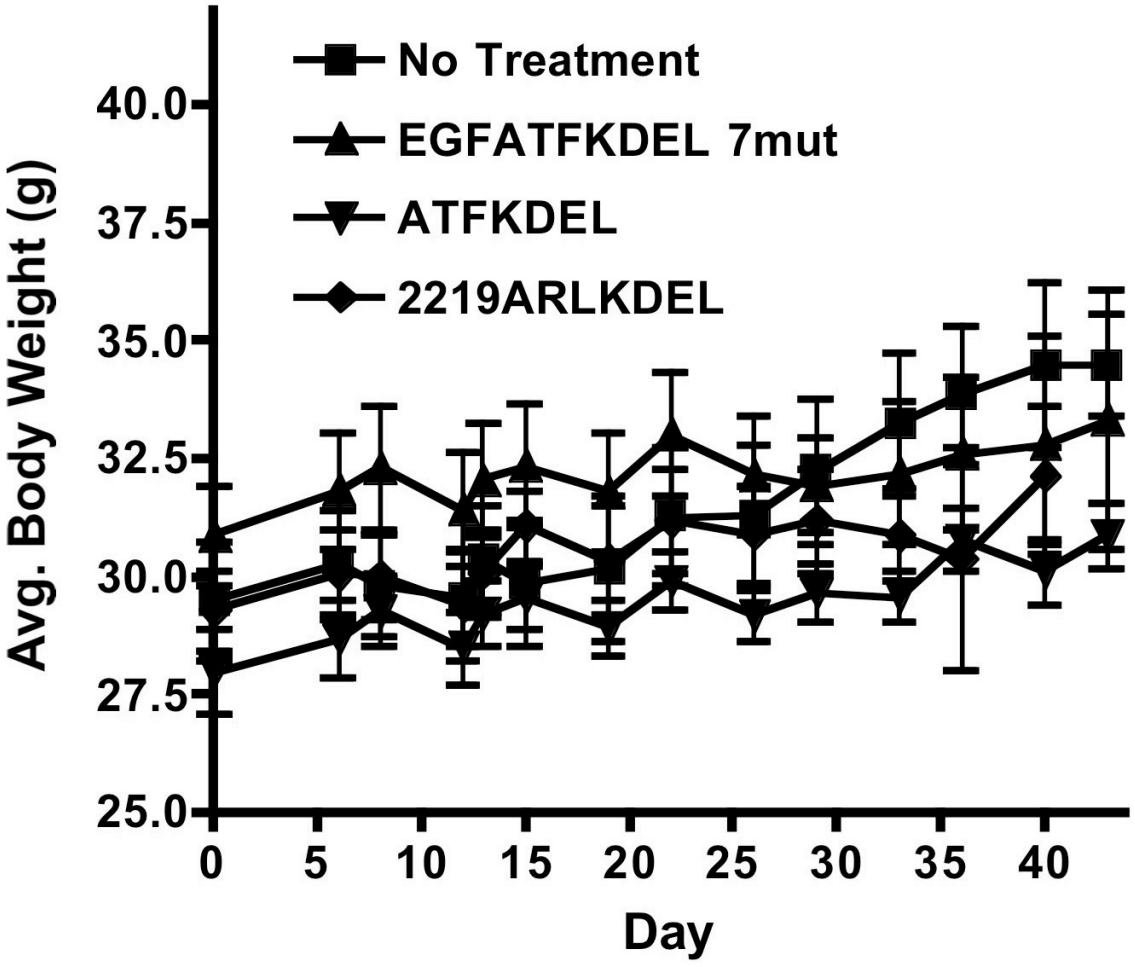

Figure 11B. Treatment associated toxicity of EGFATFKDEL 7mut, ATFKDEL, and 2219ARLKDEL administration. Body weights of mice were taken twice per week. The weights for each of the four groups were averaged.

Figure 12A

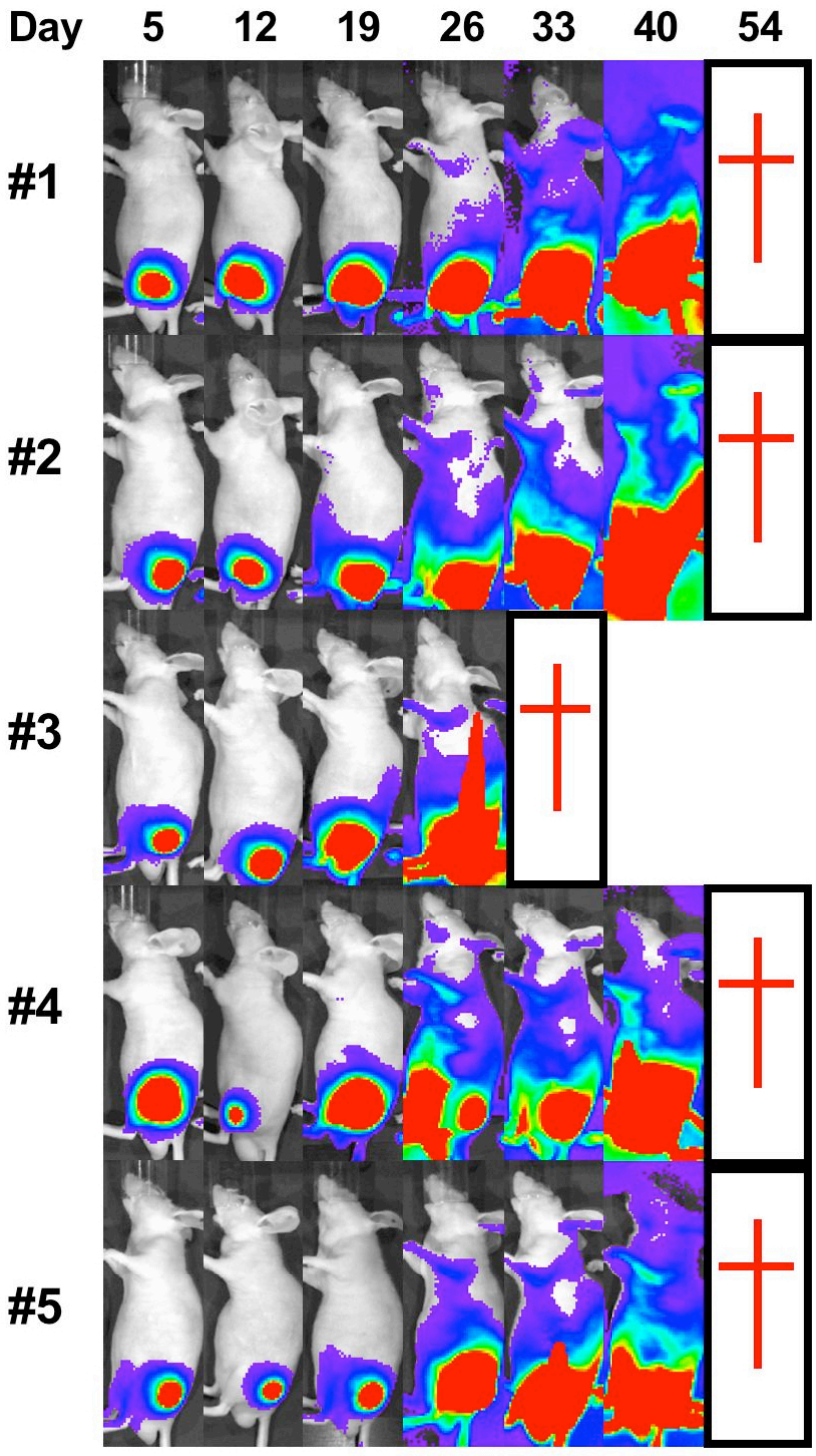

Figure 12A. Tumor growth in untreated mice. Bioluminescent images were taken of individual mice once per week. The first group was not treated after inoculation with U87-Luc cells (n=5). Crosses indicate death or euthanization.

Figure 12B

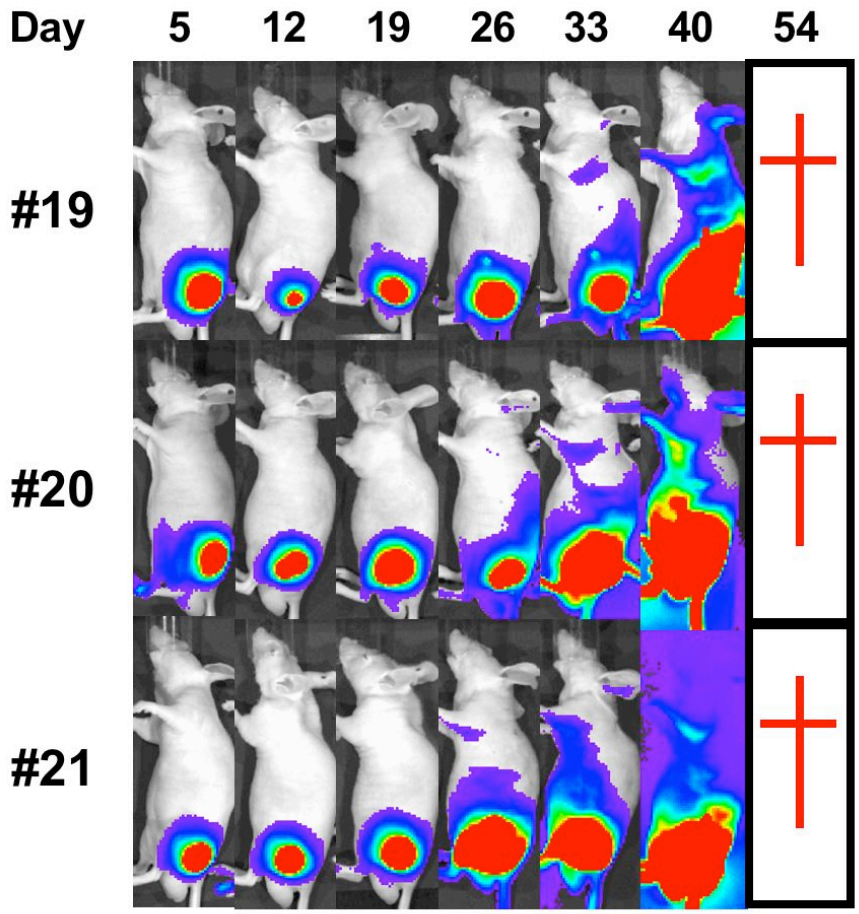

Figure 12B. Tumor growth in mice treated with 2219ARLKDEL. Bioluminescent images were taken of individual mice treated with negative control 2219ARLKDEL (n = 3). Crosses indicate death or euthanization.

Figure 12C

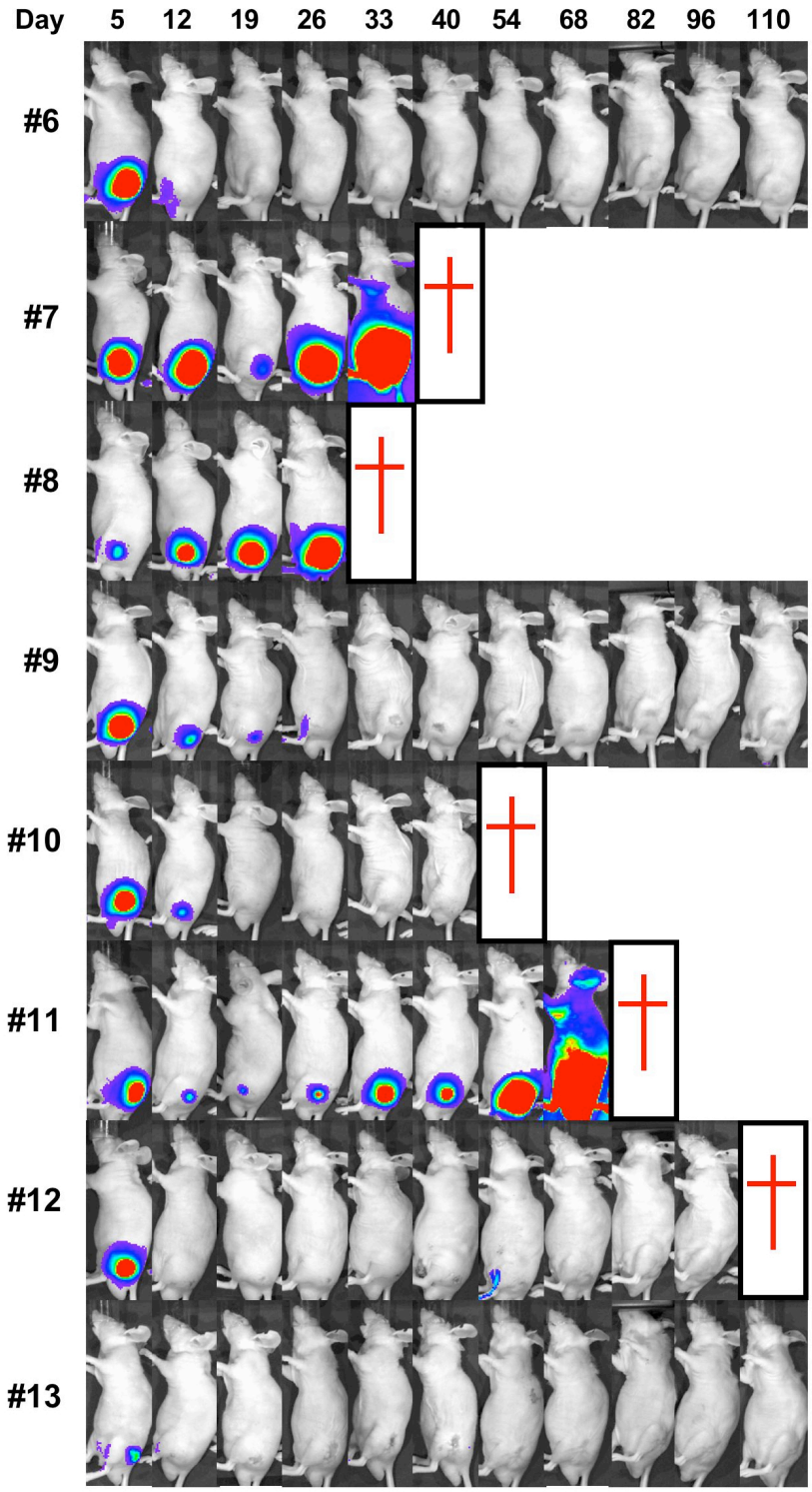

Figure 12C. Tumor regression in mice treated with EGFATFKDEL 7mut. Bioluminescent images were taken of individual mice treated with EGFATFKDEL 7mut (n = 8). Long-term survivors were maintained past day 110. Crosses indicate death or euthanization.

Figure 13A

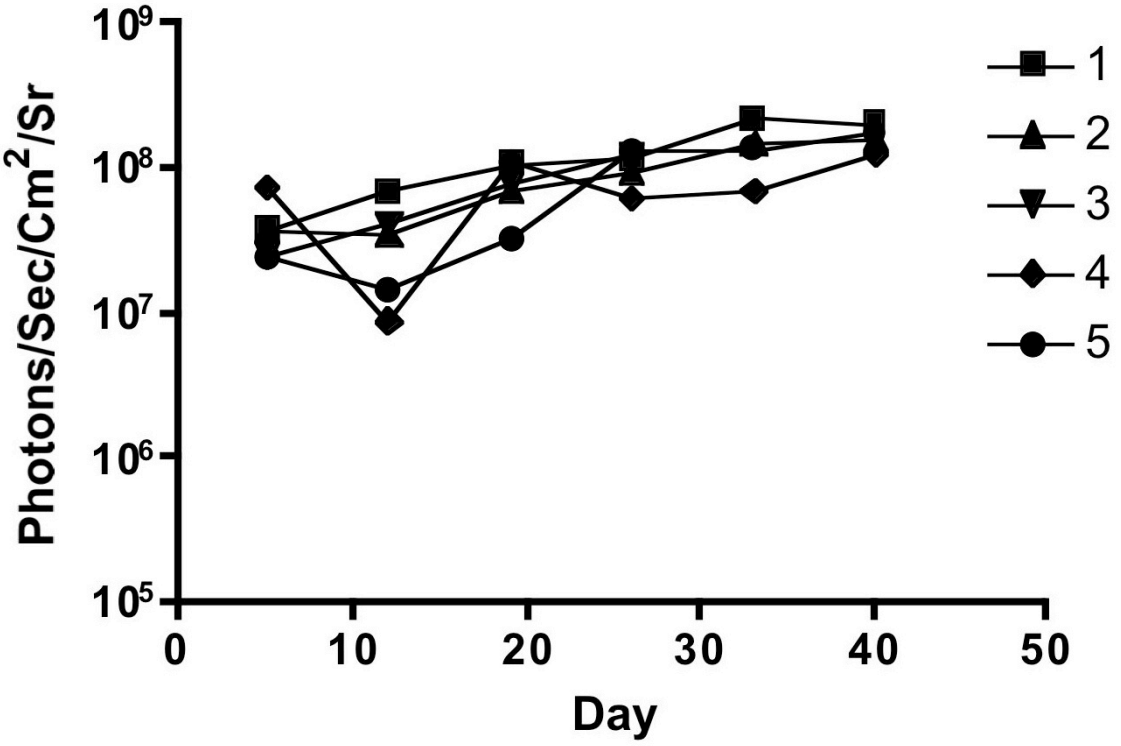

Figure 13A. Total photon tumor activity of the individual untreated mice. The amount of luciferase bioluminescence was measured during imaging of untreated mice. Bioluminescence was measured in photons/sec/cm^2/sr. The numbers represent individual mice in the no treatment group.

Figure 13B

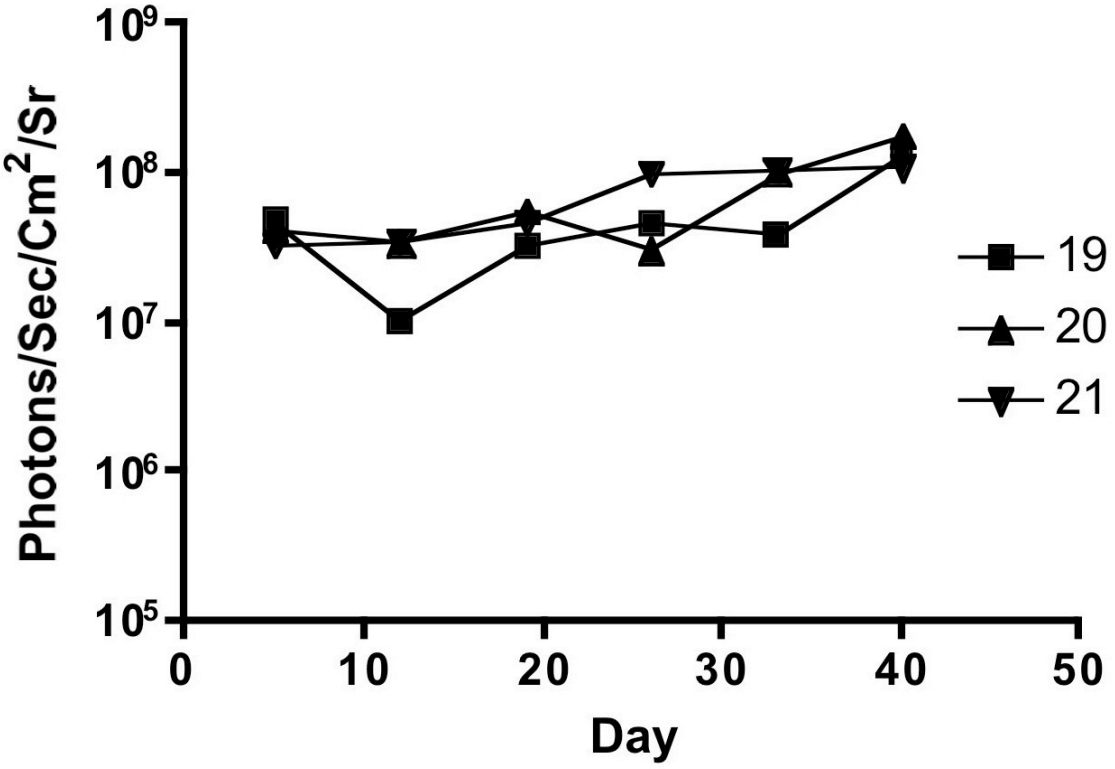

Figure 13B. Total photon tumor activity of the individual mice treated with 2219ARLKDEL. The amount of luciferase bioluminescence was measured during imaging of mice treated with negative control 2219ARLKDEL. Bioluminescence was measured in photons/sec/cm^2/sr. The numbers represent individual mice in the treatment group.

Figure 10C

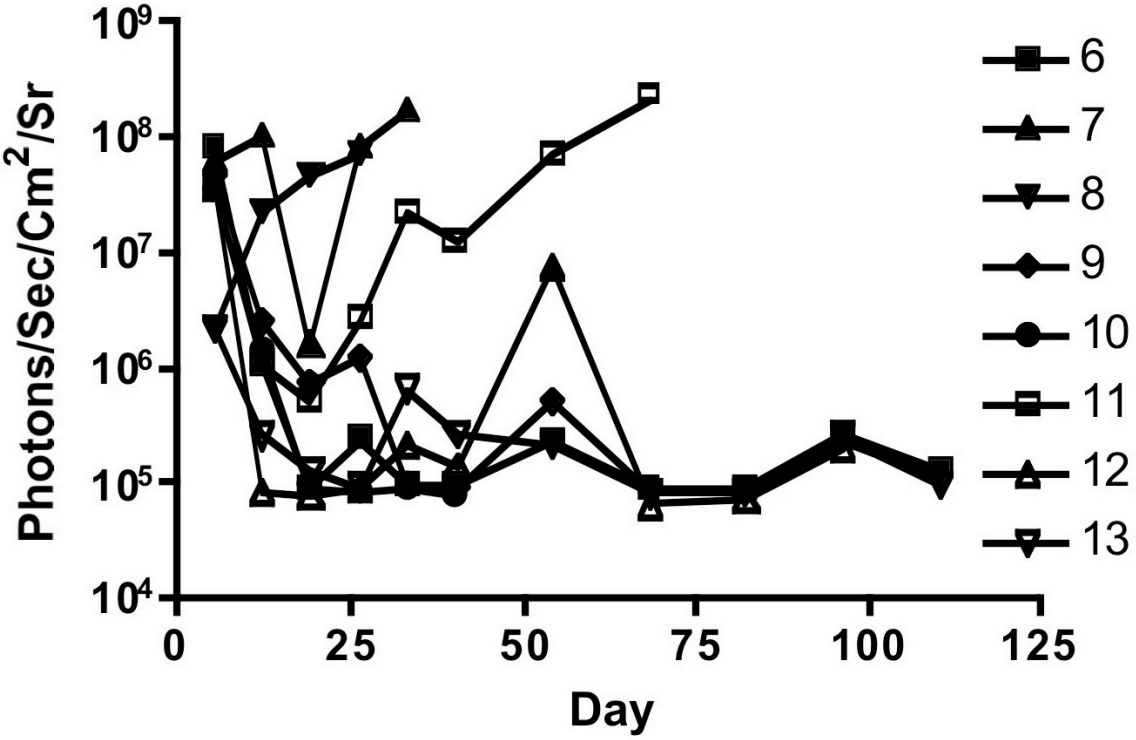

Figure 13C. Total photon tumor activity of the individual mice treated with EGFATFKDEL 7mut. The amount of luciferase bioluminescence was measured during imaging of mice treated with EGFATFKDEL 7mut. Bioluminescence was measured in photons/sec/cm^2/sr. The numbers represent individual mice in the treatment group.

Figure 13D

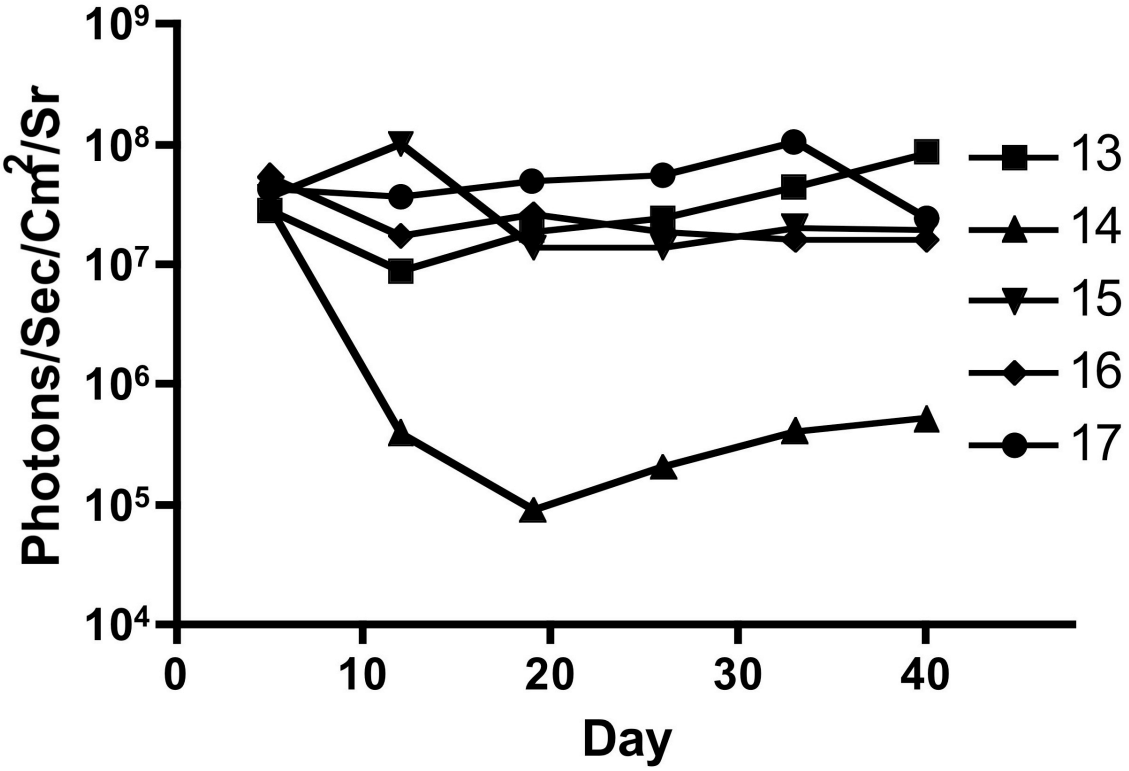

Figure 13D. Total photon tumor activity of the individual mice treated with ATFKDEL. The amount of luciferase bioluminescence was measured during imaging of mice treated with ATFKDEL. Bioluminescence was measured in photons/sec/cm^2/sr. The numbers represent individual mice in the treatment group.

Discussion

The original contribution of this research is the development and evolution of a promising new anti-glioblastoma agent with potential for clinical development. The most recent drug, EGFATFKDEL 7mut, is a unique, deimmunized bispecific drug with both anti-tumor and anti-angiogenic properties. Importantly, this novel drug showed potent anti-GBM activity and has an improved clinical outlook when compared to previous generations of TT.

Our laboratory has designed and published BLTs which simultaneously bind to dual independent receptors on the surface of tumor cells[19,21-26]. However, the toxins described here (DTEGFATF, EGFATFKDEL, and EGFATFKDEL 7mut) are the first targeted toxins that simultaneously attack tumor cells and the blood supply that feeds them. Angiogenesis, or generation of neovasculature, is a complex process which involves several elements including endothelial cells, stromal cells, and factors from the extracellular matrix. There has been tremendous interest in drugs which target the neovasculature[11]. For example, bevacizumab and other anti-angiogenic drugs currently in clinical trials have demonstrated that the vasculature can be successfully targeted with antibodies and other neovasculature targeting strategies[11]. Although angiogenesis inhibitors possess impressive potential, their success has been limited mostly by the fact that tumor regressions are often only partial[11]. Due to the limitations in other anti-angiogenics, we were particularly interested in comparing ATFKDEL, which primarily targets tumor neovasculature, with EGFATFKDEL 7mut, which targets both the tumor and its neovasculature. Our findings with ATFKDEL, in which the drug limited tumor

growth but did not induce complete remissions in 4 of 5 or 80% of the mice, correlate with the previously discussed limitations. Since EGFATFKDEL directly attacks the most prominent cells in the tumor (vascular cells and tumor cells), we believe that when compared to other anti-angiogenic drugs, our drug's effects will be magnified because the toxic effect of PE is catalytic and irreversible, and because of the drug's unique dual targeting.

Another advantage to bispecific TTs is that they allow targeting of a greater breadth of tumor cells. Cell heterogeneity is common in tumors of virtually all types, so targeting of multiple markers common on the majority of cells is advantageous. In gliomas, EGFR is amplified on 40-50% of cases, while uPAR appears to be overexpressed in most tumors but at variable levels[59,95]. Heterogeneity of these receptors in individual tumors is undoubtedly high. Consequently, as opposed to monospecific TTs, use of bispecific EGFATFKDEL 7mut means that each toxin molecule can be directed toward a malignant cell which expresses EGFR, uPAR, or both. In this particular case with EGFATFKDEL 7mut, targeting using EGF and ATF results in the ability to target three cell types: EGFR-positive tumor cells, uPAR-positive tumor cells, and uPAR-positive neovasculature.

The *in vitro* method used here to test EGFATFKDEL 7mut's ability to target the neovasculature relies on HUVECs – a human endothelial cell line. The results with HUVECs demonstrate that EGFATFKDEL 7mut can potentially impact tumor neovasculature. However, because HUVECs do not identically resemble tumor neovasculature, our findings with HUVECs are not necessarily an accurate reflection of the effect of this drug on tumor neovasculature. Nonetheless, while it should be

acknowledged that HUVECs are not an optimal model of tumor neovasculature, our studies show that the ATF portion of our drug was effectively targeting uPAR on endothelial cells. The *in vivo* data supports this because it demonstrates that EGFATFKDEL 7mut is highly effective in a mouse model in which flank tumors were induced by the injection of the human glioblastoma line U87. Tumor-free survivors were observed beyond day 110, despite the fact that treatment ended on day 40, indicating that drug responses were durable.

Other properties that set EGFATFKDEL 7mut apart from other biological targeted toxins are its toxin modifications. First, the KDEL sequence was added to the C-terminus. This modification dramatically enhances toxin potency by increasing the ability for PE molecules to reach the ER where they can translocate to the cytosol and interact with EF2[84]. In TT development, diphtheria toxin has often been chosen instead of PE due to its increased cytotoxicity. Because deimmunization is currently only available with PE, the KDEL modification has been an important technique to increase PE's cytotoxicity to levels comparable to DT. However, the KDEL modification does not necessarily result in an increased therapeutic window and it is possible that the advantage of increased potency may be negated by enhanced toxicity. To address this issue, KDEL-modified EGFATF 7mut could be compared to non-KDEL modified EGFATF 7mut in future studies. Increased toxicity due to KDEL modification of PE cannot, however, explain why EGFKDEL killed mice while EGFATFKDEL did not. We have observed that monospecific EGFKDEL is at least a log more toxic than bispecific EGFATFKDEL and we are currently determining whether this is related to the smaller size of EGFKDEL and consequent kidney filtration.

Another, more important toxin modification was the "deimmunization" of EGFATFKDEL 7mut. Kreitman et al. showed that the clinical efficacy of treatment with targeted toxins against solid tumors hinges on the ability to give multiple treatments or sustained treatment which enables the drug to penetrate a solid tumor[80]. Toxins may be administered locally to treat tumors in sensitive organs, but targeted toxins must still be used repeatedly or via sustained delivery to achieve positive results. The major problem with this is that neutralizing antibodies will be generated that significantly reduce efficacy over time. To address this issue, investigators used an expansive library of anti-PE monoclonal antibodies to epitope map prominent molecular regions which elicited the strongest antibody response. Fortunately, the immunogenic regions of PE were isolated to seven distinct epitotic areas, and not distributed throughout the molecule. We constructed our PE-based BLT and mutated key amino acids in each of the seven regions without compromising toxin activity. The immune response to the resultant second-generation drug was reduced by 80-90% in a validated mouse model[86]. This, in theory, should enable prolonged treatment with the drug without loss in efficacy due to patient immune responses.

Our immunization experiments are designed to evoke gradual immune responses by administering low concentrations of drug on a weekly basis. Initial responses are mild, but they grow exponentially, as seen in Figure 7. Responses likely could be expedited by using a more aggressive immunization regimen employing greater dosages and more immunizations. However, from other studies we know that neutralizing antibodies are present when anti-toxin levels reach about 500 μg/ml. Consequently, analysis of early and low antibody production is important. In our experiments, anti-toxin levels in some

mice treated with the parental drug exceeded this threshold after only four injections (day 26). After eight injections, none of the mice treated with the mutant drug had reached 20% of this threshold. However, it is possible that extending the experiment beyond day 62 could reveal that the response to the mutant is delayed and not eliminated. Regardless of whether or not the mutated PE fragment eventually generates an immune response, it is clear that the potential duration for EGFATFKDEL 7mut treatment is far greater than with unmutated EGFATFKDEL.

Another concern of our mouse immunogenicity studies is that major histocompatibility complex (MHC) haplotypes differ in their presentation of peptide fragments in the MHC groove and a different haplotype might present different peptides. In other words, basic immunology dictates that a danger of mutating B cell recognizing regions of the toxin is that peptides regarded as immunogenic by one MHC polymorphism, may not be regarded as immunogenic by a different polymorphism. Thus, we used two mice strains, BALB/c and C57BL/6, with entirely different MHC haplotypes. We observed significant anti-toxin reductions in both strains, indicating that the strength of mutating all seven regions was enough to overcome differences in MHC polymorphisms. However, if the remaining anti-toxin response cannot be eliminated by future mutation of other B cell recognizing amino acids, we may need to pursue mutation of the T cell recognizing toxin regions.

A final concern of the immunogenicity studies is whether mice are useful for studying human anti-toxin responses. Kreitman and Pastan have treated over 300 patients with non-mutated PE targeted toxins[94]. Nagata studied the antibodies in patients with high titers of anti-PE antibodies and found they bind to the same seven epitopes which

regulate toxin B cell recognition in mice indicating that mice are a useful model for human anti-PE responses[94].

Interestingly, we have observed that toxin mutation (deimmunization) significantly increases the activity of EGFATFKDEL 7mut, but not other BLT[21]. Onda et al. noted that certain toxin mutations enhanced the activity of one targeted toxin as well[86]. In these instances, different toxin mutation combinations were compared, but only one ligand was explored. There are several explanations which can possibly account for changes in toxin activity, but we favor binding as the most likely reason. Binding has a major impact on the activity of targeted toxins[96]. Any mutation can affect positions of alpha helices, beta strands, and turns. This consequentially impacts tertiary protein configuration and these shifts can improve binding. Sequence variances can also affect refolding quality during protein synthesis which can also affect binding. This could explain why mutation of EGFATFKDEL enhances activity, but mutation of EGF4KDEL does not[26].

Regarding binding, our flow cytometry data indicated that the bispecific drug was superior to its monospecific counterparts due to increased binding. While maximum binding was observed at 1000 nM, these high concentrations are unrealistic for clinical use, and the data shown at lower concentrations more accurately compare binding rates between the monospecifics and bispecific. These findings correlated with our *in vivo* studies which showed that the monospecific forms were not as effective at dosages comparable to the bispecific drug.

There are other potential issues when applying findings from mouse studies to humans. In humans, we do not know whether treatments will be separated by days or weeks or how the disruption of the blood-brain barrier (BBB) by tumor and surgery may

expedite immunologic recognition. We do know that antitoxin antibodies developed in a surprisingly high proportion of 73% of CED patients in phase 1 clinical studies where patients received intracranial IL-13 spliced to the same (unmutated) pseudomonas exotoxin used in our studies[88].Also, now that we know PE can be deimmunized, some will argue that any additional clinical trials should be performed with deimmunized PE. (The same way that most clinical trials are no longer performed without humanizing antibodies.) Knowing that we can now reduce the anti-toxin response at least 80% without significantly affecting toxin activity, we believe that deimmunization will be necessary in all future trials.

Our *in vivo* experiments showed that in a mouse flank tumor model, EGFATFKDEL 7mut was impressively effective against GBM tumors. Treatment of eight mice yielded five tumor-free mice, four of which were long-term survivors. Although flank tumor models are useful for determining drug efficacy against vascularized tumors, they are not ideal. For our study, drug was injected directly into small, palpable, and established tumors because targeted toxins have been vigorously pursued for IC therapy in which they are delivered directly into the tumor. A more sophisticated model would use controlled IC delivery via CED in which drug is pumped through a catheter directly into the brain tumor[7-9]. This is an established model in our laboratory and these studies are underway[26]. Initial results using this model in rats have been positive. CED treatment delayed tumor growth in the vast majority of rats, and ultimately cured nearly half of the treatment group. The use of luciferase bioluminescence in the flank tumor model presented here has been crucial for our future studies of EGFATFKDEL 7mut. We have shown that a high degree of correlation exists

between tumor volume and luciferase bioluminescence. This observation is particularly important for our current IC CED model in which tumor size cannot be directly measured.

A final concern of the flank tumor models presented above rests in the cells used. U87 is a highly aggressive GBM cell line of human origin which has a high take rate in the orthotopic xenograft model – a model which has been well established[97]. The primary concern of U87 tumors is that, histologically, they are not as invasive as GBM tumors from human patients, and consequently may be more susceptible to some treatments compared to tumors in patients[97]. Furthermore, tumor invasiveness is one of the most important characteristics in the study of angiogenesis[98]. We are currently considering other models specifically to study the anti-angiogenic nature of our drug.

Another delivery option that will require further exploration is systemic delivery. Normally, drugs of EGFATFKDEL 7mut's size would be unable to cross the BBB to reach malignant cells. However, due to its vascular reactivity, the drug may be highly effective systemically because of its ability to disrupt the BBB. Additionally, treatment in conjunction with hyperosmolar mannitol may enhance the drug's BBB disruptive capabilities. Presently, similar strategies involve the use of anti-angiogenics to disrupt the BBB in order to enhance delivery of chemotherapeutics to the brain. However, the interactions between anti-angiogenics and chemotherapeutic agents can be complicated, and conflicting results have been observed when adopting this strategy[12].

A final strategy to improve the efficacy of EGFATFKDEL 7mut involves targeting of brain cancer-propagating cells (BCPC). Stem cells have recently become popular targets for cancer therapy because they are often believed to be responsible for

drug resistance and tumor recurrence[99]. In gliomas, research suggests that BCPCs are also involved in angiogenesis, invasion, and metastasis[99]. Consequently, eliminating BCPCs may be an important step in GBM therapy with EGFATFKDEL 7mut to ensure complete tumor regression and long-term remission. Genetic analysis of BCPCs has revealed a number of different biological pathways which are important in BCPC differentiation. Thus, one strategy to reduce BCPC is to employ agents which activate these pathways and lead to stem cell differentiation[99]. Another strategy involves targeting of BCPCs using neural stem cell markers such as Nestin and CD133. Our laboratory is currently developing a CD133-based TT which could potentially be administered in conjunction with EGFATFKDEL 7mut to target progenitor cells, the tumor neovasculature, and the tumor itself. While we did not observe recurrence in any of our tumor-free mice, the necessity for a BCPC-targeting drug will depend on results from more advanced animal models, and potentially future clinical trials.

In summary, we have shown that EGFATFKDEL 7mut is effective in inducing complete remissions against GBM tumors. *In vitro*, the drug is effective in the picomolar range against tumor cells and against HUVEC cells which proves that it binds vascular cells. Attempts at deimmunization of the drug have been successful with a reduction of 80-90% anti-toxin antibodies. Based on its reduced immunogenicity and *in vivo* efficacy, the drug warrants further consideration for clinical development.

Bibliography

1. Clarke J, Butowski N, Chang S. Recent advances in therapy for glioblastoma. Arch Neurol. 2010;67:279-83.

2. Lino M, Merlo A. Translating biology into clinic: the case of glioblastoma. Current Opinion in Cell Biology. 2009;21:311-16.

3. Kanu OO, Hughes B, Di C, et al. Glioblastoma multiforme oncogenomics and signaling pathways. Clin Med Oncol. 2009;3:39-52.

4. Stupp R, Mason WP, van den Bent MJ, et al. Radiotherapy plus concomitant and adjuvant temozolomide for glioblastoma. N Engl J Med. 2005;352:987-96.

5. Stupp R, Hegi ME, Mason WP, et al. Effects of radiotherapy with concomitant and adjuvant temozolomide versus radiotherapy alone on survival in glioblastoma in a randomized phase III study: 5-year analysis of the EORTC-NCIC trial. Lancet Oncol. 2009;10:459-66.

6. Heimberger AB, Sampson JH. The PEP-3-KLH (CDX-110) vaccine in glioblastoma multiforme patients. Expert Opin Biol Ther. 2009;9:1087-98.

7. Kioi M, Husain SR, Croteau D, Kunwar S, Puri RK. Convection-enhanced delivery of interleukin-14 receptor-directed cytotoxin for malignant glioma therapy. Technol Cancer Res Treat. 2006;5:239-250.

8. Laske DW, Youle RJ, Oldfield EH. Tumor regression with regional distribution of the targeted toxin TF-CRM 107 in patients with malignant brain tumors. Nat Med. 1997;3:1362-1368.

9. Hall WA, Vallera DA. Efficacy of antiangiogenic targeted toxins against glioblastoma multiforme. Neurosurg Focus. 2006;20:E23.

10. Fukumura D, Jain RK. Imaging angiogenesis and the microenvironment. APMIS. 2008;116:695-715.

11. Carmeliet P, Jain RK. Angiogenesis in cancer and other diseases. Nature. 2000;407:249-257.

12. Verhoeff JJ, van Tellingen O, Claes A, et al. Concerns about anti-angiogenic treatment in patients with glioblastoma multiforme. BMC Cancer. 2009;9:444.

13. Vallera DA, Li C, Jin N, Panoskaltsis-Mortari A, Hall WA. Targeting urokinase-type plasminogen activator receptor on human glioblastoma tumors with diphtheria toxin fusion protein DTAT. J Nat Cancer Inst. 2002;94:597-605

14. Kreitman RJ. Recombinant immunotoxins containing truncated bacterial toxins for the treatment of hematologic malignancies. BioDrugs. 2009;23:1-13.

15. Schmidt M, Hynes NE, Gronder B, et al. A bivalent single-chain antibody-toxin specific for ErbB-2 and the EGF receptor. Int J Cancer. 1996;65:538-46.

16. Duke-Cohen JS, Morimoto C, Schlossman SF. Depletion of the helper/inducer (memory) T cell subset using a bispecific antibody-toxin conjugate directed against CD4 and CD29. Transplantation. 1993;56:1188-96.

17. Shen GL, Li JL, Vitetta ES. Bispecific anti-CD22/anti-CD3-ricin A chain immunotoxin is cytotoxic to Duadi lymphoma cells but not T cells in vitro and shows both A-chain-mediated and LAK-T-mediated killing. J Immunol. 1994;152:2368-76.

18. Kriangkum J, Xu B, Nagata LP, et al. Bispecific and bifunctional single chain recombinant antibodies. Biomolecular Engineering. 2001;18:31-40.

19. Vallera DA, Stish BJ, Shu Y, et al. Genetically designing a more potent anti-pancreatic cancer agent by simultaneously cotargeting human IL-13 and EGF receptors in a mouse xenograft model. Gut. 2008;57:634-41.

20. Oh S, Ohlfest JR, Todhunder DA, et al. Intracranial elimination of human glioblastoma brain tumors in nude rats using the bispecific ligand-directed toxin, DTEGF13 and convection enhanced delivery. J Neurooncol. 2009;95:331-42.

21. Stish BJ, Oh S, Chen H, Dudek AZ, Kratzke RA, Vallera DA. Design and modification of EGF4KDEL 7mut, a novel bispecific ligand-directed toxin, with decreased immunogenicity and potent anti-mesothelioma activity. Br J Cancer. 2009;101:1114-1123.

22. Stish BJ, Chen H, Shu Y, Panoskaltsis-Mortarti A, Vallera DA. A bispecific recombinant cytotoxin (DTEGF13) targeting human IL-13 and EGF receptors in a mouse xenograft model of prostate cancer. Clin Cancer Res. 2007;13:6486-6493.

23. Stish BJ, Chen H, Shu Y, Panoskaltsis-Mortari A, Vallera DA. Increasing anticarcinoma activity of an anti-erbB2 recombinant immunotoxin by the addition of an anti-EpCAM sFv. Clin Cancer Res. 2007;15:3058-3067.

24. Vallera DA, Todhunter DA, Kuroki DW, Shu Y, Sicheneder A, Chen H. A bispecific recombinant immunotoxin, DT2219, targeting human CD19 and CD22 receptors in a mouse xenograft model of B-cell leukemia/lymphoma. Clin Cancer Res. 2005;11:3879-3888.

25. Vallera DA, Todhunter D, Kuroki DW, Shu Y, Sicheneder A, Panoskaltsis-Mortari A, Vallera VD, Chen H. Molecular modification of a recombinant, bivalent anti-human CD3 immunotoxin (Bic3) results in reduced *in vivo* toxicity in mice. Leuk Res. 2005;29:331-341.

26. Oh S, Stish BJ, Sachdev D, Chen H, Dudek AZ, Vallera DA. A novel reduced immunogenicity bispecific targeted toxin simultaneously recognizing human epidermal growth factor and interleukin-4 receptors in a mouse model of metastatic breast carcinoma. Clin Cancer Res. 2009;15:6137-6147.

27. Taylor JM, Cohen S, Mitchell WM. Epidermal growth factor: high and low molecular weight forms. Proceedings of the National Academy of Science. 1970;67:164-71.

28. Savage CR, Hash JH, Cohen S. Epidermal growth factor, location of disulfide bonds. Journal of Biological Chemistry. 1973;248:7669-72.

29. Voldborg BR, Damstrup L, Spang-Thomsen M, et al. Epidermal growth factor receptor (EGFR) and EGFR mutations, function and possible role in clinical trials. Annals of Oncology. 1997;8:1197-1206.

30. Cohen S, Carpenter G, King Jr. L. Epidermal growth factor-receptor-protein kinase interactions. Journal of Biological Chemistry. 1980;255:4834-42.

31. Rusch V, Mendensohn J, Dmitrovsky E. The epidermal growth factor receptor and its ligands as therapeutic targets in human tumors. Cytokine & Growth Factor Reviews. 1996;7:133-41.

32. Halatsch M, Schmidt U, Behnke-Mursch J, et al. Epidermal growth factor receptor inhibition for the treatment of glioblastoma multiforme and other malignant brain tumours. Cancer Treatment Reviews. 2006;32:74-89.

33. Marti U, Burwen SJ, Wells A, et al. Localization of epidermal growth factor receptor in hepatocyte nuclei. Hepatology. 1991;13:15-20.

34. Cao H, Lei Zm, Bian L, et al. Functional nuclear epidermal growth factor receptors in human choriocarcinoma JEG-3 cells and normal human placenta. Endocrinology. 1995;136:3163-72.

35. Lin S, Makino K, Xia W, et al. Nuclear localization of EGF receptor and its potential new role as a transcription factor. Nature Cell Biology. 2001;3:802-8.

36. Lo H, Hung M. Nuclear EGFR signalling network in cancers: linking EGFR pathway to cell cycle progression, nitric oxide pathway and patient survival. British Journal of Cancer. 2006;94:184-8.

37. Arnold D, Seufferlein T. Targeted treatments in colorectal cancer: state of the art and future perspectives. Gut. 2010;59:838-58.

38. Yoshida T, Zhang G, Haura EB. Targeting epidermal growth factor receptor: central signaling kinase in lung cancer. Biochem Pharmacol. 2010;80:613-23.

39. Alvarez RH, Valero V, Hortobagyi GN. Emerging targeted therapies for breast cancer. J Clin Oncol. 2010;28:3366-79.

40. Ekstrand AJ, Sugawa N, James CD, et al. Amplified and rearranged epidermal growth factor receptor genes in human glioblastomas reveal deletions of sequences encoding portion of the N- and/or C-terminal tails. Proc Natl Acad Sci. 1992;89:4309-4313.

41. Fontanini G, Vignati S, Bigini D, et al. Epidermal growth factor receptor (EGFr) expression in non-small cell lung carcinomas correlates with metastatic involvement of hilar and mediastinal lymph nodes in the squamous subtype. Eur J Cancer. 1995;31:178-83.

42. Neal DE, Marsh C, Bennett MK, et al. Epidermal-growth-factor receptors in human bladder cancer: comparison of invasive and superficial tumours. Lancet. 1985;1:366-8.

43. Mukaida H, Toi M, Hirai T, et al. Clinical significance of the expression of epidermal growth factor and its receptor in esophageal cancer. Cancer. 1991;68:142-8.

44. Nicholson S, Richard J, Sainsbury C, et al. Epidermal growth factor receptor (EGFr); results of a 6 year follow-up study in operable breast cancer with emphasis on the node negative subgroup. Br J Cancer. 1991;63:146-50.

45. Oxnard GR, Miller VA. Use of erlotinib or gefitinib as initial therapy in advanced NSCLC. Oncology (Williston Park). 2010;24:392-9.

46. Fakih M, Wong R. Efficacy of the monoclonal antibodyFR inhibitors for the treatment of metastatic colorectal cancer. Current Oncology. 2010;17:S3-S17.

47. Ochenduszko SL, Krzemieniecki K. Targeted therapy in advanced colorectal cancer: more data, more questions. Anticancer Drugs. 2010;21:737-48.

48. Liu TF, Tatter SB, Willingham MC, et al. Growth factor receptor expression varies among high-grade gliomas and normal brain: epidermal growth factor receptor has excellent properties for interstitial fusion protein therapy. Molecular Cancer Therapy. 2003;2:783-7.

49. Sampson JH, Akabani G, Archer GE. Progress report of a phase I study of the intracerebral microinfusion of a recombinant chimeric protein composed of transforming growth factor (TGF)-alpha and a mutated form of the pseudomonas exotoxin termed PE-38 (TP-38) for the treatment of malignant brain tumors. J Neurooncol. 2003;65:27-35.

50. Mondino A, Blasi F. uPA and uPAR in fibrinolysis, immunity and pathology. Trends Immunol. 2004;25:450-5.

51. Henic Emir, Borgfeldt C, Christensen IJ, et al. Cleaved forms of the urokinase plasminogen activator receptor in plasma have diagnostic potential and predict postoperative survival in patients with ovarian cancer. Clin Cancer Res. 2008;14:5785-93.

52. Moller LB. Stucture and function of the urokinase receptor. Blood Coagulation and Fibrinolysis. 1993;4:293-303.

53. Choong PF, Nadesapillai AP. Urokinase plasminogen activator system: a multifunction role in tumor progression and metastasis. Clin Orthop Relat Res. 2003;415:S46-58.

54. Bugge TH, Flick MJ, Danton MS, et al. Urokinase-type plasminogen activator is effective in fibrin clearance in the absence of its receptor or tissue-type plasminogen activator. Proc Natl Acad Sci. 1996;93:5899-904.

55. Abraham E, Gyetko MR, Kuhn K, et al. Urokinase-type plasminogen activator potentiates lipopolysaccharide-induced neutrophil activation. J Immunol. 2003;170:5644-51.

56. Hoyer-Hansen G, Ploug M, Behrendt N, et al. Cell-surface accerleration of urokinase-catalyzed receptor cleavage. Eur J Biochem. 1997;243:21-6.

57. Andolfo A, English WR, Resnati M, et al. Metalloproteases cleave the urokinase-type plasminogen activator receptor in the D1-D2 linkner region and expose epitopes not present in the intact soluble receptor. Thromb Haemost. 2002;88:298-306.

58. Blasi F. Urokinase and urokinase receptor: a paracrine/autocrine system regulating cell migration and invasiveness. BioEssays. 1993;15:105-11.

59. Lakka SS, Gondi CS, Rao JS. Proteases and glioma angiogenesis. Brain Pathol. 2005;15;327-41.

60. Nykjaer A, Moller B, Todd RF, et al. Urokinase receptor. An activation antigen in human T lymphocytes. J Immunol. 1994;152:505-16.

61. Bianchi E, Ferrero E, Fazioli F, et al. Integrin-dependent induction of functional urokinase receptors in primary T lymphocytes. J Clin Invest. 1996;98:1133-41.

62. Plesner T, Behrendt N, Ploug M. Structure, function and expression on blood and bone marrow cells of the urokinase-type plasminogen activator receptor, uPAR. Stem Cells. 1997;15:398-408.

63. Blasi F. The urokinase receptor. A cell surface regulated chemokine. APMIS. 1999;107:96-101.

64. Gyetko MR, Sud S, Chen GH, et al. Urokinase-type plasminogen activator is required for the generation of a type 1 immune response to pulmonary Cryptococcus neoformans infection. J Immunol. 2002;168:801-9.

65. Stonehouse TJ, Woodhead VE, Herridge PS, et al. Molecular characterization of U937-dependent T-cell co-stimulation. Immunology. 1999;96:35-47.

66. Woodhead VE, Stonehouse TJ, Binks MH, et al. Novel molecular mechanisms of dendritic cell-induced T cell activation. Int Immunol. 2000;12:1051-61.

67. Gyetko MR, Sud S, Chensue SW. Urokinase-deficient mice fail to generate a type 2 immune response following schistosomal antigen challenge. Infect Immun. 2004;72:461-7.

68. Sebastio G, Riccio A, Verde P, et al. BamHI RFLP linked to the human urokinase gene. Nucleic Acids Res. 1985;13:5404

69. Stoppelli MP, Corti A, Soffientini A, et al. Differentiation-enhanced binding of the amino-terminal fragment of human urokinase plasminogen activator to a specific receptor on U937 monocytes. Proc Natl Acad Sci. 1985;82:4939-43.

70. Cubellis MV, Nolli ML, Cassani G, et al. Binding of single-chain prourokinase to the urokinase receptor of human U937 cells. J Biol Chem. 1986; 261:15819-22.

71. Rustamzadeh E, Hall WA, Todhunter DA, *et al*. Intracranial therapy of glioblastoma with the fusion protein DTAT in immunodeficient mice. Int J Cancer. 2006;120:411-419.

72. Binder BR, Mihaly J, Prager GW. uPAR-uPA-PAI-1 interactions and signaling: a vascular biologist's view. Thromb Haemost. 2007;97:336-42.

73. Kroon ME, Koolwijk P, van der Vecht B, et al. Urokinase receptor expression on human microvascular endothelial cells is increased by hypoxia: implications for capillary-like tube formation in a fibrin matrix. Blood. 2000;96:2775-83.

74. Mori T, Abe T, Wakabayashi Y, et al. Up-regulation of uroinase-type plasminogen activator and its receptor correlates with enhanced invasion activity of human glioma cells mediated by transforming growth factor-alpha or basic fibroblast growth factor. J Neurooncol. 2000;46:115-23.

75. Ulisse S, Baldini E, Sorrenti S, et al. The urokinase plasminogen activator system: a target for anti-cancer therapy. Current Cancer Drug Targets. 2009;9:32-71.

76. Riisbo R, Christensen IJ, Piironen T, et al. Prognostic significance of soluble urokinase plasminogen activator receptor in serum and cytosol of tumor tissue from patients with primary breast cancer. Clin Cancer Res. 2002;8:1132-41.

77. Stephens RW, Nielsesn HJ, Christensen IJ, et al. Plasma urokinase receptor levels in patients with colorectal cancer: relationship to prognosis. J Natl Cancer Inst. 1999;91:869-74.

78. Bell CE, Poon PH, Schumaker VN, et al. Oligomerization of a 45 kilodalton fragment of diphtheria toxin at pH 5.0 to a molecule of 20-24 subunits. Biochemistry. 1997;36:15201-7.

79. Yamaizumi M, Mekada E, Uchida T, et al. One molecule of diphtheria toxin fragment A introduced into a cell can kill the cell. Cell. 1978;15:245-50.

80. Kreitman RJ, Stetler-Stevenson M, Margulies I, *et al*. Phase II trial of recombinant immunotoxin RFB4(dsFv)-PE38 (BL22) in patients with hairy cell leukemia. J Clin Onc. 2009;27:2983-2990.

81. Kreitman RJ, Pastan I. Accumulation of a recombinant immunotoxin in a tumor in vivo: fewer than 1000 molecules per cell are sufficient for complete responses. Cancer Res. 1998;58:968-75.

82. Chaudhary VK, Jinno Y, Fitzgerald D, et al. Pseudomonas exotoxin contains a specific sequence at the carboxyl terminus that is required for cytotoxicity. Proc Natl Acad Sci. 1990;87:308-12.

83. Kreitman RJ, Pastan I. Importance of the glutamate residue of KDEL in increasing the cytotoxicty of pseudomonas exotoxin derivatives and for increased binding to the KDEL receptor. Biochem J. 1995;307:29-37.

84. Hessler JL, Kreitman RJ. An early step in Pseudomonas exotoxin action is removal of the terminal lysine residue, which allows binding to the KDEL receptor. Biochemistry. 1997;36:14577-82.

85. Onda M, Nagata S, FitzGerald DJ, *et al*. Characterization of the B cell epitopes associated with a truncated form of Pseudomonas exotoxin (PE38) used to make immunotoxins for the treatment of cancer patients. J Immunol. 2006;177:8822-8834.

86. Onda M, Beers R, Xiang L, Nagata S, Wang Q, Pastan I. An immunotoxin with greatly reduced immunogenicity by identification and removal of B cell epitopes. *PNAS.* 2008;105:11311-11316.

87. Hassan R, Bullock S, Premkumar A, *et al*. Phase I study of SS1P, a recombinant anti-mesothelin immunotoxin given as a bolus I.V. infusion to patients with mesothelin-expressing mesothelioma, ovarian, and pancreatic cancers. Clin Cancer Res. 2007;13:5144-5149.

88. Vogelbaum MA, Sampson JH, Kunwar S, *et al*. Convection-enhanced delivery of cintredekin besudotox (interleukin-13-PE38QQR) followed by radiation therapy with and without temozolomide in newly diagnosed malignant gliomas: phase 1 study of final safety results. Neurosurgery. 2007;61:1031–1037.

89. Studier FW, Moffatt BA. Use of bacteriophage T7 RNA polymerase to direct selective high-level expression of cloned genes. J Mol Biol. 1986;189:113-30.

90. Vallera DA, Chen H, Sicheneder AR, Panoskaltsis-Mortari A, Taras EP. Genetic alteration of a bispecific ligand-directed toxin targeting human CD19 and CD22 receptors resulting in improved efficacy against systemic B cell malignancy. Leuk Res. 2009;33:1233-1242.

91. Bancroft CC, Chen Z, Yeh J, et al. Effects of pharmacologic antagonists of epidermal growth factor receptor, PI3K and MEK signal kinases on NF-kappaB and AP-1 activation and IL-8 and VEGF expression in human hea and neck squamous cell carcinoma lines. Int J Cancer. 2002;99:538-48.

92. Vallera DA, Ash RC, Zanjani ED, Kersey JH, LeBien TW, Beverley PC, Neville DM Jr, Youle RJ. Anti-T-cell reagents for human bone marrow transplantation: ricin linked to three monoclonal antibodies. Science. 1983;222:512-515.

93. Vallera DA, Taylor PA, Sprent J, Blazar BR. The role of host T cell subsets in bone marrow rejection directed to isolated major histocompatability complex class I versus class II differences of bm1 and bm12 mutant mice. Transplantation. 1994;57:249-256.

94. Nagata S, Pastan I. Removal of B cell epitopes as a practical approach for reducing the immunogenicity of foreign protein-based therapeutics. Adv Drug Deliv Rev. 2009;61:977-985.

95. Eppenberger U, Mueller H. Growth factor receptors and their ligands. J Neurooncol. 1994;22:249-54.

96. Ho M, Nagata S, Pastan I. Isolation of anti-CD22 Fv with high affinity by Fv display on human cells. Proc Natl Acad Sci U S A. 2006;103:9637-42.

97. de Vries NA, Beijnen JH, van Tellingen O. High-grade glioma mouse models and their applicability for preclinical testing. Cancer Treatment reviews. 2009;35:714-23.

98. Goldrunner RH, Wager S, Roosen K, et al. Models for assessment of angiogenesis in gliomas. J Neurooncol. 2000;50:53-62.

99. Van Meir EG, Hadjipanayis CG, Norden AD, et al. Exciting new advances in neuro-oncology: the avenue to a cure for malignant glioma. Ca Cancer J Clin. 2010;60:166-93.